HIGHLIGHTING THE HISTORY OF FRENCH RADIO ASTRONOMY. 6: THE MULTI-ELEMENT GRATING ARRAYS AT NANÇAY

Monique Pick and Jean-Louis Steinberg
Paris Observatory (Meudon), Place Jules Janssen, F-92 195 Meudon Cedex, France.
E-mails: Monique.Pick@obspm.fr; chapias1922@orange.fr

Wayne Orchiston
Centre for Astronomy, James Cook University, Townsville, Queensland 4811, Australia.
E-mail: Wayne.Orchiston@jcu.edu.au

and

André Boischot
5 bis rue d'Arsonval, 75015 Paris, France.
E-mail: boischot.andre@wanadoo.fr

Abstract: After constructing a number of simple antennas for solar work at Nançay field station, during the second half of the 1950s and through into the 1960s radio astronomers from the Paris Observatory (Meudon) erected five different innovative multi-element arrays. Three of these operated at 169 MHz, a fourth at 408 MHz and the fifth array at 9,300 MHz. While all of these radio telescopes were used for solar research, one of the 169 MHz arrays was used mainly for galactic and extra-galactic research. In this paper we discuss these arrays and summarise the science that was achieved with them during this important period in the development of French radio astronomy.

Keywords: French radio astronomy, solar radio emission, Nançay, multi-element arrays, A. Boischot, É.-J. Blum, J.-F. Denisse, M. Pick, J.-L. Steinberg.

1 INTRODUCTION

French involvement in radio astronomy has a long history, dating back to Nordmann's unsuccessful attempt to detect solar radio emission at 0.3-3 MHz from Grands-Mulets in the Alps in 1901. However, the earliest positive developments only took place in the years immediately following WW II when a fledgling radio astronomy group at the École Normale Supérieure led by Jean-François Denisse and Jean-Louis Steinberg carried out research from the roof of the Physics Building in Paris and from a field station located at Marcoussis, 20 km south of Paris.

In 1952 Marius Laffineur (Institute of Astrophysics, Paris) and Jean-Louis Steinberg attended the URSI Congress in Sydney, Australia, where they saw the innovative radio telescopes developed by scientists from the CSIRO's Division of Radiophysics at the Dapto, Hornsby Valley and Potts Hill field stations.[1] Steinberg was particularly impressed by the E-W solar grating array that Chris Christiansen had developed at Potts Hill. This instrument was the first one to produce high resolution observations of the distribution of 1420 MHz radio emission across the solar disk. The array consisted of 32 aerials arranged in an E-W straight line at uniform spacings; the combined response of the array produced a series of fan-shaped beams. The design of this instrument and the main observational results were recently reviewed in this journal by Wendt et al. (2008).

Steinberg returned to Paris convinced that French radio astronomy needed a radio-quiet field station and similar arrays. This was the genesis of the Nançay field station, 190 km south of Paris.[2]

After the transfer of the Radio Astronomy group from the École Normale Supérieure to Paris Observatory (Meudon), solar and non-solar research began at Nançay with two recycled 7.5m ex-German WWII Würzburg antennas (Orchiston et al., 2007)[3] and a number of smaller dishes, some of which were configured as interferometers. Kundu's two element interferometer was the first one to use Earth rotation synthesis to produce a one-dimensional distribution of solar radio emission (see Orchiston et al., 2009).

The next major development in French radio astronomy occurred in the second half of the 1950s when three different multi-element arrays designed principally for solar research were constructed at Nançay.

This paper reviews the technical specifications of these three instruments and other multi-element grating arrays that were developed at that site a little later, and the associated scientific research.[4] In addition to the personal involvement of three of the authors of this paper (MP, J-LS and AB), we discuss the work of the following colleagues: Yvette Avignon, Constantin Caroubalos, Bernard Clavelier, Jean-François Denisse, Anne-Marie Malinge-Le Squeren, Michel Moutot, Gérard Trottet, Émile-Jacques Blum, Michel Ginat, Mohan Joshi, Pierre Lantos, Yolande Leblanc, Paul Simon and Marc Vinokur. Regrettably, the last seven colleagues are no longer with us, but Émile-Jacques Blum was looking forward to participating in this project and had he survived he would certainly have been a co-author of this paper. He died on 22 September 2009, and we would like to dedicate this paper to his memory.

The instruments discussed in this paper were constructed and operated with the participation of the following technical staff: Claude Chantelat (deceased), Michel and Yvette Chapuis, Christian Couteret, Alain Gerbault, Jean-François Mangin, Marcele Parise (deceased) and Roland Tocqueville.
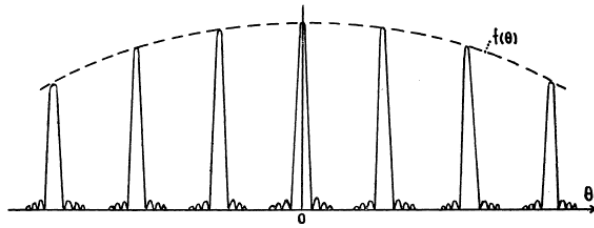
Figure 1: Radiation pattern of an E-W grating array.

2 THE CONSTRUCTION OF THE ARRAYS AT NANÇAY

2.1 Introduction

Major developments of French solar radio astronomy started with the founding of the Nançay field station in 1953. This site offered for the first time in France the possibility of developing arrays with long baselines, and E-W grating arrays operating at 169 MHz, 408 MHz and 9300 MHz were built. They were meridian instruments and their principle was similar to that of the 1,420 MHz Potts Hill array built by Christiansen and Warburton (1953) in Australia. Identical antennas were distributed at equal spacings along an E-W axis and their signals were added using transmission lines with equal electrical lengths. In hour angle this produced a series of 'fringes' (fan beams), which were equally spaced near the meridian plane (see Figure 1). A periodic one-dimensional image was obtained through the motion of the source across the fringes due to the rotation of the Earth.

Another meridian array was also constructed, but it had 8 antennas that were spaced along a N-S baseline (Maligne et al., 1959). This array operated at 169 MHz, but in contrast to the E-W arrays the motion of the source at noon was parallel to the fringes and images could only be obtained by using a multi-beam system.

2.1.1 The Principle

If $f(\alpha, \beta)$ is the reception pattern in amplitude of each individual antenna, that of a multi-element interferometer, $D(\alpha, \beta)$, is given by

$$D(\alpha, \beta) = f(\alpha, \beta) \frac{\sin n\frac{\Phi}{2}}{n \sin\frac{\Phi}{2}} \qquad (1)$$

where

$$\Phi = (2\pi d/\lambda)\sin\alpha \qquad (2)$$

and d is the distance between two neighboring antennas, n the number of antennas, λ the observing wavelength, α the angle between the line of sight and the meridian plane, and β the angle between the line of sight and the horizontal plane.

Near the meridian plane, the radiation pattern consists of a series of fan beams (see Figure 1) separated by an angle

$$\Delta\alpha = \lambda/d \qquad (3)$$

2.1.2 The 169 MHz and 408 MHz E-W Grating Arrays: A Brief History

The first array began operating in June 1956 and consisted of 8 parabolic antennas (Blum et al., 1956). These had a diameter of 5-m, meridian mountings, and were spaced at 50-m intervals. From November 1956 the array consisted of 16 antennas, and on 14 April 1957 it began observations in its final configuration (see Figure 2), with 32 antennas (Blum et al., 1957; Boischot, 1958). The operating frequency was 169 MHz (λ = 1.775 m).

In 1963, it was decided to use 16 antennas (that is, every second antenna) to build a new array working at 408 MHz, and to operate at 169 MHz with the remaining 16 antennas, keeping the same resolving power with a field of view reduced to 1° at 169 MHz, but wide enough for the radio Sun. The 408 MHz array began operating in October 1965 (see Clavelier, 1968b).

In 1968, the 16 parabolas of the E-W array working at 169 MHz were replaced by new, flat low-bandwidth antennas (diameter 3-m) with equatorial mountings, and the 408 MHz array was then operated with 32 antennas, raising the field of view to 50′. This upgraded version at 408 MHz was in operation by the end of 1972. On 2 September 1971 a fire destroyed
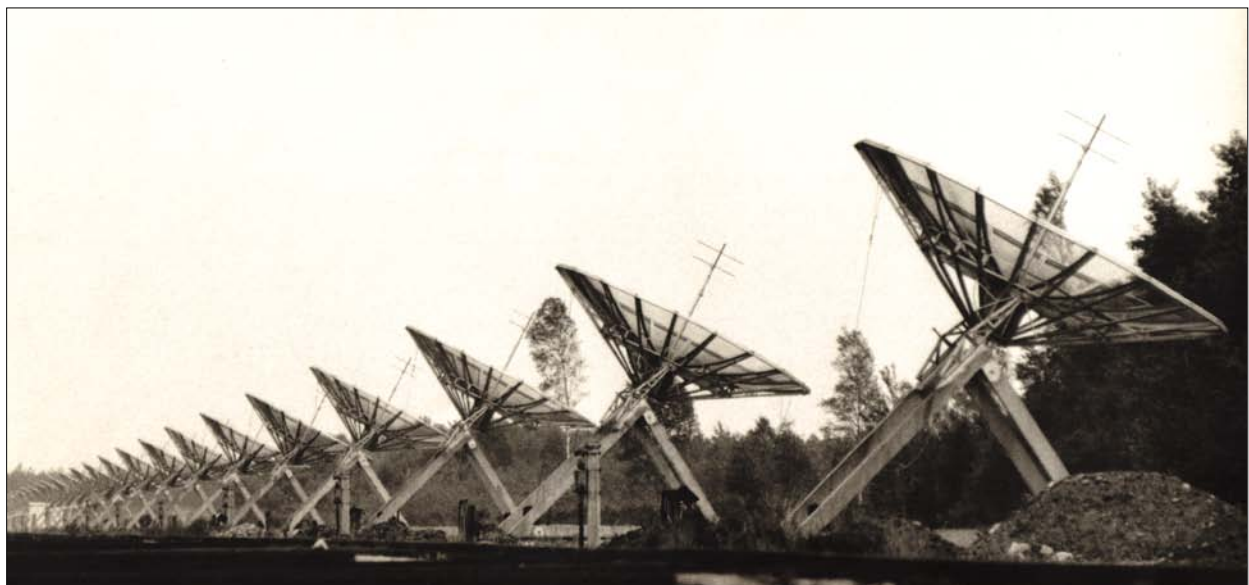

Figure 2: The 32 parabolic antennas of the E-W array.

the receiver of the 169 MHz array. The decision was then taken to develop a radioheliograph able to give a two-dimensional image of the Sun. The E-W branch of this new instrument started operating at 169 MHz in 1975.

Figure 3: Schematic diagram showing the western half of the Nançay 169 MHz E-W array.

2.2 The Initial 169 MHz E-W Array with 32 Antennas

2.2.1 The Antennas

This was a 1550-m meridian instrument with antennas spaced at equal intervals along an E-W line. Signals from the antennas were added through equal electrical lengths and produced a series of E-W fringes after quadratic detection. The resolving power was 3.8′ (in theory 3′) and the angular distance between neighbouring grating lobes was 2° 02′. The E-W orientation was accurate to ~1′. For practical reasons (ground reflections, ionospheric effects), the observations were limited to declinations of $\geq -33°$. Point sources could be located in the E-W direction with an accuracy of better than 1′.

Each antenna was a 5-m diameter parabola fed from its focus by a dipole (and its reflector). The surface was made of mesh tightened between 20 parabolic ribs that were distributed regularly around the focal axis. The surface accuracy was about ±1 cm at the centre and ±1.5 cm on the edges. A single dipole illuminated the parabola over an angle of 120°. The effective area of an antenna was ~15m^2 and the gain was 17.8 dB. The half power beam width of each antenna was ~20°.

2.2.2 The Receiver

The whole receiver used vacuum tube technology. The configuration of the interferometer is schematized in Figure 3. The signal from each dipole was fed to a coaxial cable through a transformer. The signals from consecutive neighbouring antennas were first added before being fed to a preamplifier with a gain of 50 dB (adjustable within ± 3 dB) and a band pass of 11 MHz. There were sixteen identical preamplifiers. This was the first array in radio astronomy to use a series of preamplifiers distributed along the antennas.

The signal was fed by coaxial cables of equal length to a receiver located in the central building. The receiver contained a post-amplifier to enhance the high frequency signal, a mixer with its local oscillator and an intermediate frequency amplifier at 11 MHz with a pass band of 2.5 MHz.

Radio sources were observed to determine the characteristics of the interferometer. A difficulty was to identify the crossing of the central (zero order) fan beam by the radio source. For this purpose, two other amplifiers were tuned at 11 + 0.9 MHz and 11 – 0.9 MHz respectively with a pass band of 0.7 MHz, so that the overall receiver was tuned to 169 + 0.9 MHz and 169 – 0.9 MHz. Thus, the antenna polar diagram was made of two sets of grating fan beams, but only the central fan beams coincided, giving an easy method to identify them.

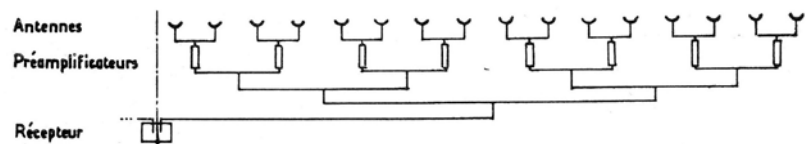Figure 4 shows observations of the discrete sources Virgo A, Hydra A and Cygnus A. As these sources are at different right ascensions, their transit times are different as well as the distances between successive beams (Blum et al., 1957). Radio source observations were used to determine the deviations in shape and position of the grating fan beams from the theoretical ones, and also to check the level of first side lobes (in principle 4.5%, but measured to be ~12%). The uncertainties in the determination of the right ascension were 15″ and 25″ for the most intense and the weakest sources respectively.

The finite width of the pass band, 2.5 MHz, produced a loss of coherency with hour angle and a progressive smearing of successive fan beams with their distance from the central one. This effect limited the observing time for the Sun to about ± 40 minutes around noon.

2.3 The 408 MHz E-W Array

The frequency 408 MHz was chosen for three reasons: (1) the increase in resolution compared to the E-W array at 169 MHz; (2) this frequency range had not yet been explored; and (3) the 406-410 MHz frequency range had been allocated to radio astronomy and thus was protected to some extent.

The resolution was 1′.7 and the accuracy in the localization of the sources in the E-W direction was 20″. The field of view (distance between consecutive grating fan beams) was 25′, which is smaller than the width of the Sun and led to an overlap of its eastern and western edges.
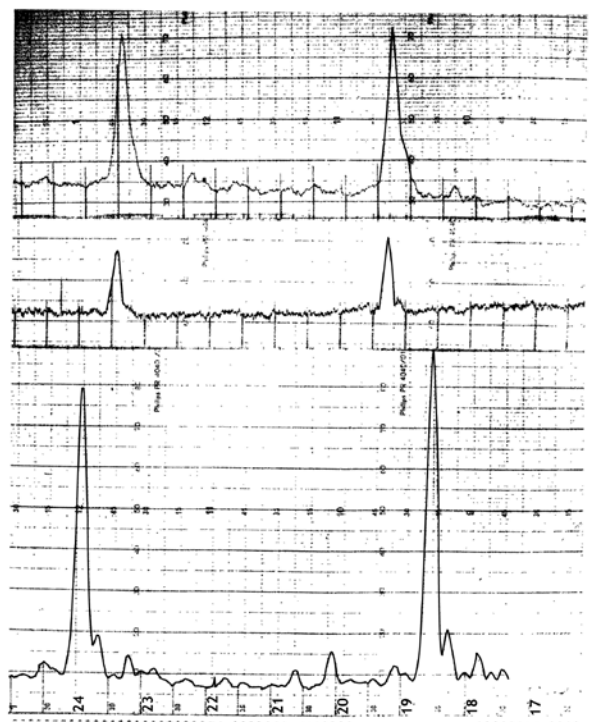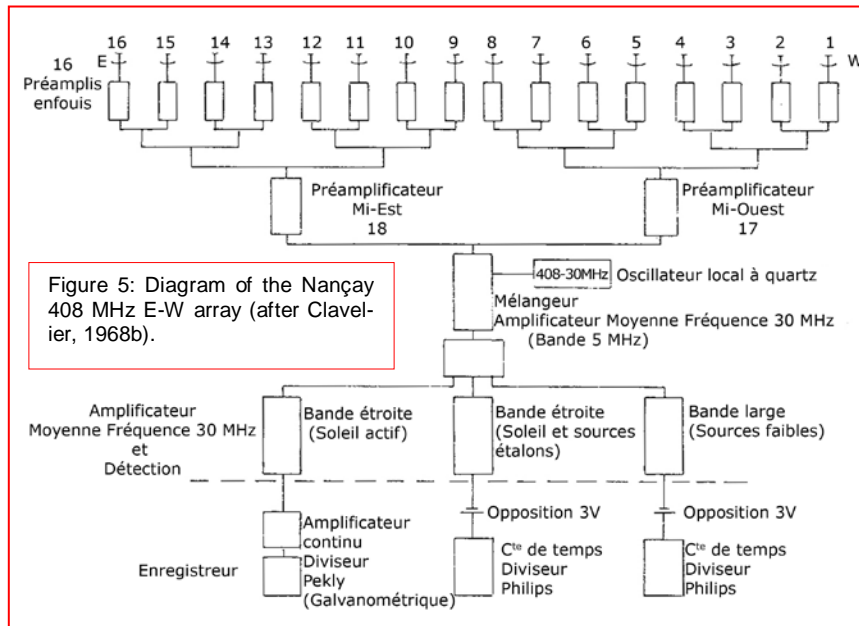

Figure 4: Records of radio sources. From top to bottom: Virgo A, Hydra A and Cygnus A. (after Blum et al., 1957).

Figure 5: Diagram of the Nançay 408 MHz E-W array (after Clavelier, 1968b).

2.3.1 The Receiver

Figure 5 shows the design of the interferometer. The main differences between it and the 169 MHz array were: (1) a preamplifier buried at a depth of 1-m close to each antenna; and (2) 'mid-east' and 'mid-west' amplifiers to compensate for the signal loss in the coaxial cables. In the central building, after a change of frequency to 30 MHz the signal was divided into three parts and sent to three amplifiers, one with a band pass of 4 MHz (used exclusively for weak calibrators) and the other two with narrower band passes of 0.4 MHz (normal observing mode) and 0.5 MHz (for bursts of short duration or high intensity).

At 408 MHz the individual antenna pattern is narrower than at 169 MHz and the observing time around noon would have been too short with fixed antennas. In order to allow observations during 1 hour around the meridian transit, a new antenna feed was developed, such that the illumination of the parabolas was only partial in the E-W (horizontal) direction; it was made of an array of two dipoles (each associated with its own linear reflector) giving an illumination of 40° and 70° at 10 dB respectively in the planes parallel and perpendicular to the dipoles. The widths of the resulting antenna patterns were 28° at 6 dB (22° at 3 dB) in the horizontal plane and 11.5° (8.5°) in the vertical plane.
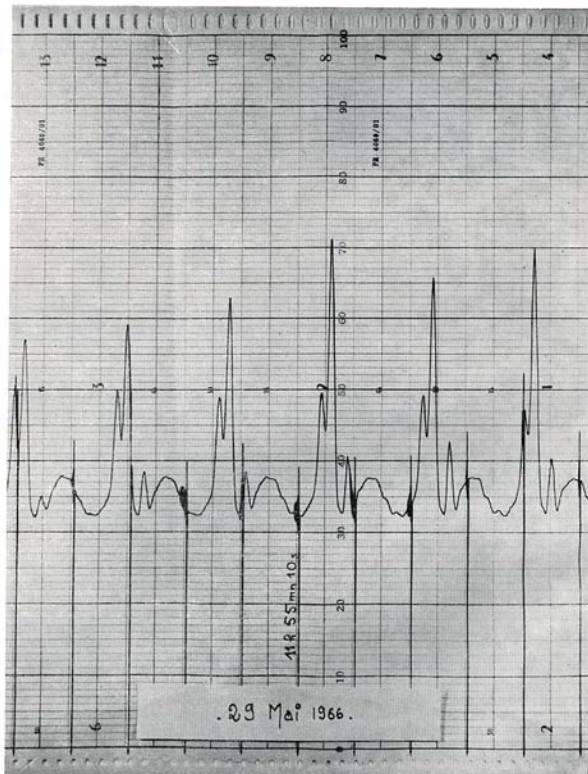
Note that for the first time in radio astronomy the preamplifiers were transistorized. In Figure 6, solar observations at 408 MHz show the presence of two active centres.

2.4 The 9300 MHz E-W Array

The 9300 MHz (λ = 3.2 cm) array was operating with eight antennas from February 1958 and with 16 antennas (Figure 7) from July 1959 (Pick and Steinberg, 1959; 1961). This radio telescope is still in operation. The sixteen antennas with filled aperture are attached to a 23-m metallic girder taken from US military radars, and are positioned at a regular spacing of 1.46-m. This girder, which is supported by four concrete piles, can be rotated around its E-W horizontal axis in order to point at various declinations. The signal is fed through waveguides to the receiver which is also supported by the girder. This avoids the use of rotating junctions, which could introduce phase variations depending on inclination (phasing must be accurate to ~10%, i.e. 3 mm).

The resolution is 4.5′ and the distance between two grating lobes is 1° 15′, much greater than the width of the Sun at this wavelength. But by using deconvolution techniques, it is possible to measure radio source diameters down to 2′.

2.4.1 The Antennas

Each antenna, which is a parabolic mirror with a diameter of 1.10-m and a focal length of 0.55-m, is illuminated by a horn. In order to increase the observing time (as for the 408 MHz array), horns have a width larger than their height and illuminate only the central part of the mirror in the E-W direction. This results in an E-W beam width of 7°, which allows an observing time of about 45 minutes. The waveguide is curved from the horn, and then crosses the reflector. The junctions by pairs have a Y shape. To avoid energy losses and phase variations due to moisture, waveguides were filled with nitrogen under pressure. Glass windows were inserted between the horns and the wave guides.

Figure 6: Record at 408 MHz of a solar radio source exhibiting two components (after Clavelier, 1967).

The impedances were matched by means of screws inserted in the wave guides. The standing wave ratio is ≤1.1 in a band pass of 100 MHz. Observations of the Sun were used to achieve the phasing of the array. When using only two neighboring antennas (putting absorbing masks in front of all of the other ones), the Sun can be considered as a point source and produces a sine wave. The shift between its meridian transit time and the time of maximum of the central fringe provides the phase correction to be applied to the antenna pair. This correction is made by inserting pieces of dielectric material in the waveguides. The side lobes level is ≤10%.

2.4.2 The Receiver

The original receiver was a super-heterodyne with an intermediate frequency of 34 MHz and a 10 MHz band pass. Its noise factor was 8 dB and its noise temperature 1500°. The same metal box contained the mixer, the local oscillator and the IF preamplifier. This box was mounted on the girder. The main amplifier and the power supply were located in the cabin.

2.5 Construction of the Multibeam Arrays at Nançay

2.5.1 The Multibeam N-S Array at 169 MHz

A new multi-beam N-S array was built in 1960 (Joshi, 1962) (see Figure 8). It was designed mainly to measure the declinations of more than one hundred radio sources during their transit in the central beam of the E-W grating array. This instrument also observed the Sun until 1964.

The N-S array contained eight 10-m parabolic dishes at 110-m spacings. The distance between grating lobes was 55.2′, and the half-power beam width was 7′. The signal from each antenna was amplified and then transmitted to the central laboratory by buried coaxial cables (see Figure 9).

These signals were then mixed with that of a local oscillator. The outputs of the mixers were 2 MHz-wide frequency bands centred at 11.55 MHz. These eight bands were sent to eight delay lines made of coaxial cables, which allowed choosing the direction of the central grating lobe. Each band was fed to an amplifier with 15 outputs. Finally, there were 15 sets of 8 intermediate frequency bands. Each set was sent to a delay line system, and the 8 outputs were added. These 15 systems pro-

Figure 7: The Nancay 9300 MHz E-W array.

Figure 8: The 8 parabolic antennas of the N-S array.

duced 15 grating lobes which were shifted by 1/16 of the grating lobe spacing: the spacing between the grating lobes was filled with the 15 shifted lobes (Figure 9). The 169 MHz output of the E-W array was mixed with the same local oscillator, and the intermed-
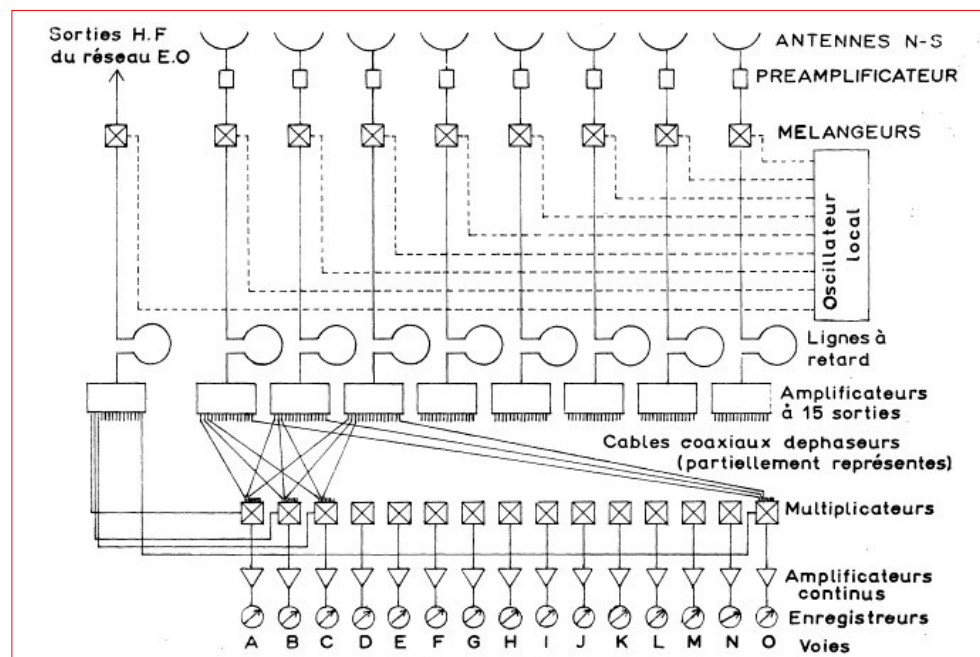

Figure 9: Diagram of the Nançay 169 MHz N-S multi-beam array and multi-channel receiver (after Joshi, 1962).
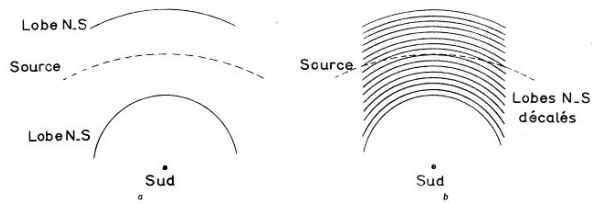
Figure 10: Two main lobes of the multi-beam N-S array. Left: A source crossing the meridian between two successive beams will be not recorded. Right: A series of beams shifted from the position of the main beam. The sources crossing the meridian will be recorded (after Joshi, 1962).

iate frequency voltage was multiplied by the fif-teen outputs of the N-S array. The 15 resulting signals were plotted on three 5-channels recorders. The lobes of the instrument on the celestial sphere are repre-sented in Figure 10. Note that a radio source was recorded only when it appeared both in an E-W and a N-S lobe (see Figure 11).
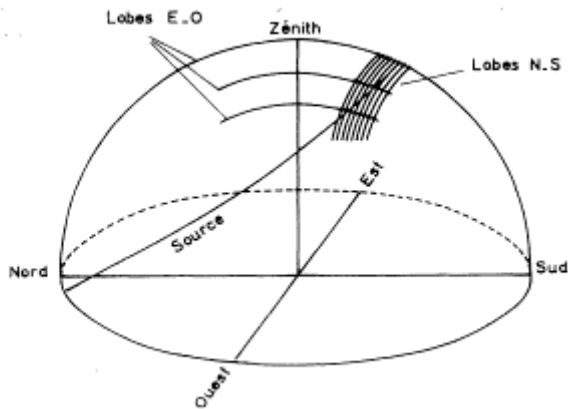

Figure 11: The lobes of the E-W and N-S arrays on the celestial sphere and the transit of the radio source in the lobes (after Joshi, 1962).

Figure 12 shows the transit of the radio source Hydra A: the source appeared in channels I and J, and its coordinates could be determined. For each trace, intensity is shown as a function of time. The position-al accuracy of the system was estimated as 1 second in hour angle and 1′ in declination, which were rather good values at that time.

Figure 12: Transit of the radio source Hydra A in a few successive beams of the N-S multichannel array: the source is culminating between lobes I and J (after Joshi, 1962).

2.5.2: The Multibeam E-W Array at 169 MHz

With the remaining 16 antennas of the 169 MHz array, an E-W multi-beam array was constructed and has been in operation since July 1967 (Vinokur, 1968). The principle of this instrument was comparable to that of the N-S array (see the previous Section). Its main achievement was the high rate and the short exposure times of the resulting picture on film which could be as fast as 1/160 second (ibid.). Figure 13 shows an example of storm burst activity, where one can see variations of bursts faster than 1/20 second. On 2 September 1971 a fire destroyed the cabin and all of the receivers.

3 SOLAR RESEARCH AT NANÇAY WITH THE THREE ARRAYS AT 9300, 408 AND 169 MHz

3.1 Introduction

Observations at different frequencies sample different heights and physical conditions in the solar atmo-sphere, with lower frequencies coming from higher levels above the photosphere. Therefore, by operating at different frequencies the Nançay arrays provided a powerful way of studying the quiet Sun and the disturbed Sun and investigating the association be-tween radio bursts and energetic solar particles in order to understand solar-terrestrial relations. The multi-frequency approach chosen by Blum, Denisse and Steinberg turned out to be fully justified, as illustrated below.

It is worth mentioning that the main goal of the large Nançay E-W array was to study noise storms, which were recognized as a type of activity that was more stable and more permanent than other types of solar radio burst emission (see Blum et al., 1957). The 150-200 MHz frequency range appeared as the most favorable for this study (Benoit, 1956). Blum et al. (1957; our translation) emphasized

> … the importance of identifying, for the study of solar-terrestrial relations, the positions of the active centres, and particularly those which were associated with radio emission.

Monthly maps from the Nançay array were published in the *Solar Geophysical Data on Solar Activity* from 1957 until October 1990, and these showed the position and intensity of the 169 MHz noise storm centres.

At 9300 MHz, the magnitude of the flux density of the 'radio condensations' associated with sunspot groups was very early on recognized as an efficient indicator of up-coming flare activity (see Section 3.2.1) and, until recently, daily messages reporting these flux density values were sent from Nançay to the Centre de Prévision de l'Activité Solaire et Géo-magnétique de l'Observatoire de Paris-Meudon, which was the regional centre of the International URSIgram and World Data Service.

Historically, solar radio emission has been divided into three categories: (1) emission from the quiet Sun; (2) the slowly varying component (SVC) which is thermal in origin and is associated with the transit of various optical features across the solar disk; and (3) sporadic activity, including a large variety of bursts.

3.2 The Quiet Sun

The level of emission from the quiet Sun at a given frequency is usually masked by the SVC-emitting sources. However, it is possible to determine the base level of emission by subtracting the SVC emissions. This was first demonstrated by Christiansen and Warburton (1953). The method adopted was to super-impose a number of daily one-dimensional profiles and to draw their lower envelopes. The same technique was applied to the Nançay observations.

3.2.1 9300 MHz Emission

The quiet Sun emission at 9300 MHz was first measured for a two month period during August-September 1959 (Pick and Steinberg, 1961). Figure 14 shows that the width of the quiet Sun at 9300 MHz is more or less the same as that of the optical disk, which is represented by the solid line, AB. Therefore the emission originates from a region close to the chromosphere. The brightness temperature of the quiet Sun was estimated to be ~20,000 K.

3.2.2 169 MHz and 408 MHz: The Quiet Sun Emission and its Variation with the Solar Cycle

Boischot (1958) determined the level of quiet Sun emission at 169 MHz as the lower envelope of daily observations (see Figure 15, right panel), during quiet periods (1956-1957) in the early part of the sunspot cycle. But even so, the number of days without noise storms or burst activity was limited (Boischot and Simon, 1959). At this frequency, the daily shape of the Sun can change considerably. This is illustrated in Figure 15 where individual strip scans of the Sun taken in April and July 1957 are shown respectively in the upper and the lower part of the left-hand panel. This figure also shows that relative to April, there is a significant decrease of almost 20% in the general level of emission in July.

Boischot (1958) also underlined the difficulty in determining the contribution from the different localized sources distributed over the total surface of the Sun and concluded that the error involved in defining the lowest level of the emission at 169 MHz from a limited observing period was far from negligible.

The next studies were thus performed with a larger sample of observations. Moutot and Boischot (1961) estimated the quiet Sun temperature for the 1958-1960 period assuming that the emission of the 'minimum envelope' originated in a uniformly-bright disk with a diameter measured at half power by the E-W interferometer; they found a brightness temperature of 800,000 K ± 15%.

Once the E-W and N-S arrays were both operating successfully, Avignon and Le Squeren-Malinge (1961) and Leblanc and Le Squeren (1969) investigated the shape and size of the corona at 169 MHz, and its change in the course of a solar cycle. The latter authors considered the variation of the 'quiet Sun' by taking the lowest envelope of the different curves recorded over periods of one month. Figure 16 displays the variations in the equatorial dimension of the 'quiet Sun'; the diameter was 47′ ± 2′ at the time of maximum solar activity, then it decreased between January 1960 and December 1961 to reach a minimum value of 38′ ± 1′ and thereafter remained more or less

Figure 13 (right): Storm burst activity observed with the multi-beam E-W array at 169 MHz. The vertical axis shows time, and each bright spot is illuminated for one second at intervals of two seconds. The horizontal axis shows the angle between the line of sight and the meridian plane of the array (after Vinokur, 1968).
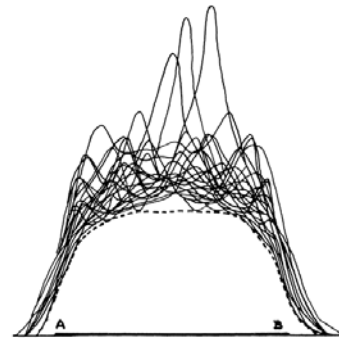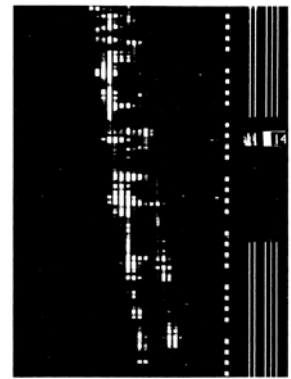

Figure 14: Superimposed individual scans of 9300 MHz emission obtained during August-September 1959, showing peaks due to 'radio plages'. Upon subtracting these, the level of quiet Sun emission (dashed line) is derived. The solid line, A-B, indicates the diameter of the optical Sun (after Pick and Steinberg, 1961: 49).
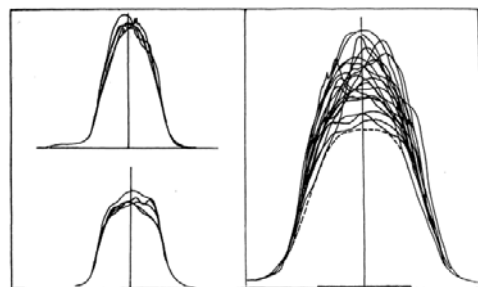

Figure 15 (left): Slow variations observed with the E-W Interferometer at 169 MHz; records obtained between 16 and 26 April 1957 (top) and 8 and 12 July 1957 (bottom). Figure 16 (right): the dotted line represents the estimated emission from the quiet Sun in 1956-1957 (after Boischot, 1958).
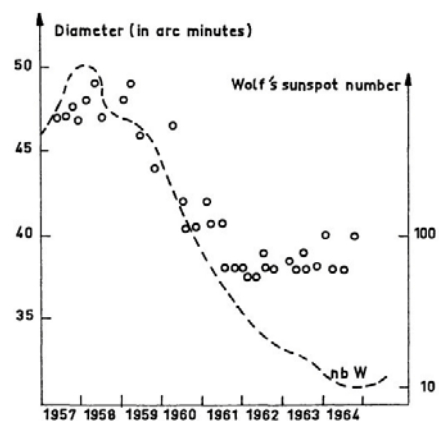

Figure 16: Apparent variations in the equatorial width of the 'Minimum Sun' (circles) during a solar cycle and variation in the Wolf sunspot number (dashed line) (after Leblanc and Le Squeren, 1969).
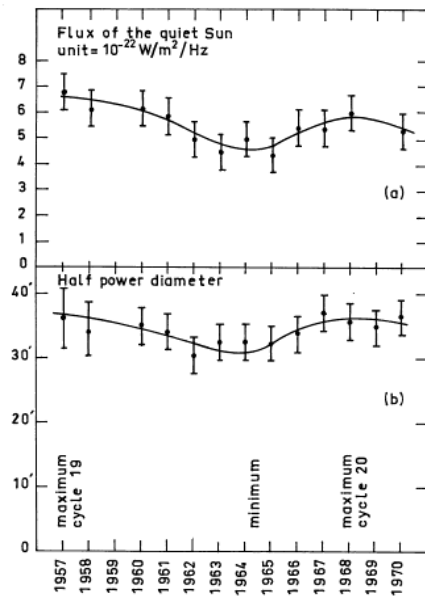
Figure 17: Flux (a) and E-W diameter at half power (b) of the radio quiet Sun at 169 MHz between 1957 and 1970 (after Lantos and Avignon, 1975).

Table 1: Values of T_b (10^5 K)

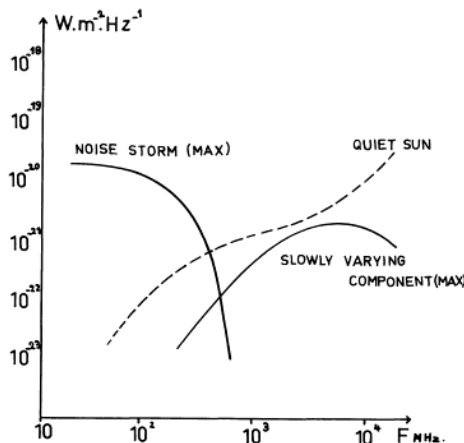| f (MHz)	T_b		Reference
	Holes	Arches	
160-169	11.5	6.3	Trottet and Lantos (1978)
160-169	6.6	8.5	Chiuderi-Drago et al. (1977)
160-169	..5.7		Dulk et al. (1977)
408	4.1	6.0	Trottet and Lantos (1978)
408	4.3	6.3	Chiuderi-Drago et al. (1977)

Figure 18: Spectra of noise storms and slowly varying components (after Clavelier, 1967).
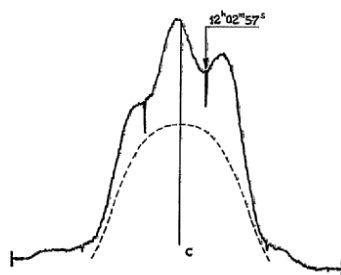

Figure 19: Scan of the Sun obtained on 7 March 1958, showing the presence of two intense radio plages (after Pick-Gutmann and Steinberg, 1959).

constant. In the same figure, the quarterly variation in Wolf sunspot numbers is plotted. It can be seen that the decrease in the E-W diameter started slightly after the beginning of the decay of the photospheric activity; the latter continued until 1964, although the diameter reached its minimum value in 1961. This suggests that the shape and size of the 'lower envelope' could still be affected until 1961 by the presence of localized sources. The N-S diameter measured from June 1960 to December 1963 was 32′ ± 3′, and no variation was found during this period. The authors, however, noticed that the limited resolving power prevented the observation of any change <6′ in this direction. The ratio of the N-S and E-W lowest dimensions of the corona gave an ellipticity of 0.84, identical to that obtained by Conway and O'Brien (1956) in 1953-1954 at 214 MHz.

Leblanc and Le Squeren found that the flux density at 169 MHz varied from $12.5 \times 10^{-22}\,\mathrm{W\,m^{-2}\,Hz^{-1}}$ at the maximum to $6.0 \times 10^{-22}\,\mathrm{W\,m^{-2}\,Hz^{-1}}$ at the time of minimum activity. The latter value corresponded to a brightness temperature of 1.1×10^6 K. The authors concluded that this temperature may be considered equal to the electron temperature in the corona, which was assumed to be optically thick at this frequency.

Finally, Lantos and Avignon (1975; cf. Avignon and Lantos, 1971) determined the dimensions, temperature and density of the solar corona for the period 1957-1970, which extends from the maximum of cycle 19 to the maximum of cycle 20. The lower envelope was defined over a year, which was the main difference with the analysis performed by Leblanc and Le Squeren (1969). Another criterion used by Lantos and Avignon (1975) was to select periods when accurate measurements of point sources were available for calibration. Figure 17 shows that the flux density and the E-W diameter have only small and simultaneous variations. It was concluded that the quiet Sun brightness temperature remains constant (T_b = 750,000 K), in agreement with measurements made by Conway and O'Brien (1956) at 214 MHz during a minimum of solar activity (T_b = 820,000 K) and with the value (800,000 K) obtained by Liu Xu Zhao and He Xiang Tao (1974) at 146 MHz.

The most interesting comparison was with the coronal holes detected at 160 MHz with the Culgoora Radioheliograph and also with the OSO 7 satellite in the 284 Å [FeXV] line by Dulk and Sheridan (1974); the brightness temperature over the radio coronal holes was 700,000K ± 20%. It was then proposed that the coronal holes seen in the far ultra-violet corresponded to the radio quiet corona as defined by the lower envelope method. It is interesting to note that this brightness temperature was comparable to the value found by Moutot and Boischot (1961) for the period 1958-1960. Avignon et al. (1975) also derived the flux density and the brightness temperature (460,000 K) of the quiet Sun at 408 MHz with the E-W Nançay array and the E-W arm of the Medicina North Cross in Italy. Again, they interpreted the lower envelop as resulting from the transit of extended coronal holes across the disk.

In 1978, Trottet and Lantos (1978) conducted a new data analysis in which they considered that the 'minimum radio quiet Sun' brightness was the result of

two distinct compon-
ents, coronal holes
and regions of closed
magnetic arches, mix-
ed in variable pro-
portions. The bright-
ness temperatures
of both components
were obtained from
one-dimensional ob-
servations with the
E-W Nançay Inter-
ferometers at 408
and 169 MHz, using
FeXV images in or-
der to estimate their
relative areas. Trottet
and Lantos (ibid.)
concluded that there
was marginal consist-
ency between the
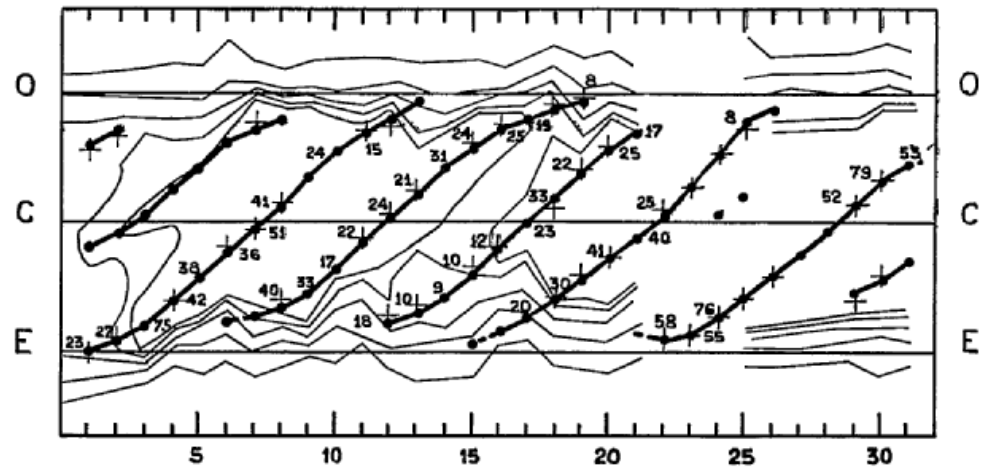radio and UV obser-
vations. Table 1 sum-
marizes the bright-

Figure 20: Map showing the evolutionary histories of individual radio plages present at 9300 MHz during March 1958. The numbers listed for the individual radio plages (black dots) are their intensities, in arbitrary units. The crosses indicate the associated optical centres. The O, C and E lines indicate the optical western limb, central meridian and eastern limb of the Sun, respectively. The series of thin lines correspond to lower level brightness contours (after Pick-Gutmann and Steinberg, 1959).

ness temperatures obtained at 160-169 MHz and 408 MHz by them and, for comparison, the values found by other studies conducted at approximately the same time.

3.3 The Slowly-Varying Component

At metre wavelengths, the solar radio flux contains a slowly varying component of thermal origin which is easily recognizable during periods without noise storms as radio flux increases (RFI's) superimposed on the quiet Sun emission (see Section 3.2). Figure 18 displays spectra of the quiet Sun, the slowly varying component (SVC) and noise storms, and shows that the SVC flux density gradually diminishes as the frequency decreases below 3 GHz (Clavelier, 1967). In the absence of noise storms, it was early realized that the sources at 169 MHz and 9300 MHz had different characteristics

3.3.1 The Slowly Varying Component at 9300 MHz

Christiansen and Mathewson (1959) showed that the SVC measured at 1420 MHz was thermal emission from active regions. This finding was confirmed at 9300 MHz by Pick and Steinberg (1961) who analyzed the Nançay observations. They found a good concord-ance between the respective daily positions of the radio plages (also called 'radio condensations') and the associated active centres. They showed that the alti-tudes of the microwave sources varied between 20,000 and 30,000 km above the photosphere (see also Gut-mann and Steinberg, 1959).

From the data obtained during March 1958, it was possible to estimate the duration, the brightness and the variations with heliographic longitude of the radio plages. Often two or even three of them were present on the Sun at any one time (see Figure 19). The motion of individual radio plages across the solar disk, and the way in which they varied in intensity during their passage is illustrated in Figure 20. Their dura-tions were typically one solar rotation.

In a study of all the optical active centres associated with radio emission observed at 9300 MHz from July

1959 to December 1963, Avignon et al. (1966) showed that the importance of this emission depended upon the magnetic structure of the centres. Figures 21 and 22 show how the parameter d/D, previously introduced by Caroubalos and Martres (1964), was chosen to de-fine the magnetic structure of the optical centre, where D is proportional to the square root of the total area of the sunspots and $2d$ is the smallest distance between two sunspots of opposite polarity. When only one spot is visible, if there is a filament close to it, such as in configuration B (bottom of Figure 21, and also Sec-tion 3.5.2), d is chosen as the distance between the spot and the filament which marks the magnetic polar-ity inversion line, otherwise d is undefined. The rela-tionship between the flux density at 9300 MHz and the total area of the spots is displayed in Figure 22. This figure shows clearly the existence of two famil-ies, the first one with a strong longitudinal magnetic field gradient ($d/D <0.2$, Categories 1 and 5) for which the flux density depends sharply on the spotted area, and the other one ($d/D >0.2$, Categories 2, 3, 4) for which this dependence is weak. For the first of these families the frequency of appearance of flares (importance >1) goes up very quickly with the area of
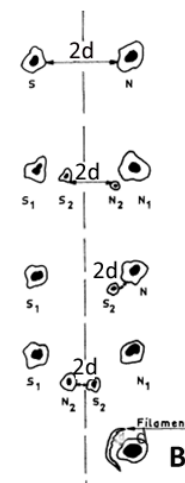

Figure 21: Measurement of parameter $2d$ (see text) (after Caroubalos and Martres, 1964).
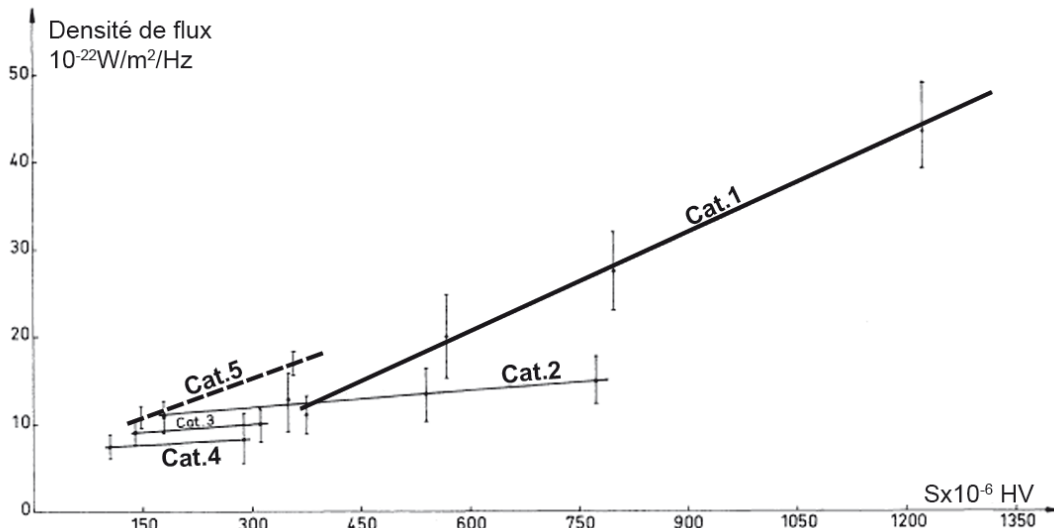
Figure 22: Variation of the flux density at 9300 MHz versus the sunspot area. Category 1: $d/D \leq 0.2$; Category 2: $0.2 < d/D \leq 1$; Category 3: $d/D > 1$; Category 4: Unipolar centres; Category 5: Centres of B configurations ≤ 0.2 see text) (after Avignon et al., 1966).

the spots. This is consistent with results found elsewhere, concerning the magnetic structure of active centres associated with cosmic rays or proton events (Ellison et al, 1962) or with Type IV bursts (see Section 3.5.2). This is also consistent with the results obtained by Moutot and Boischot (1961), who showed that active centres with an emission $>15 \times 10^{-22}$ W m^{-2}Hz^{-1} at 9300 MHz were always associated with a noise storm at metre wavelengths. It was proposed that at 9300 MHz, the sources belonging to the first family were generated by the thermal gyromagnetic emission mechanism introduced by Kakinuma and Swarup in 1962.
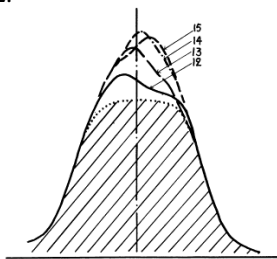

Figure 23: Sources of emission of the slowly varying component seen for four successive days in May 1958. The authors' estimate of the level of quiet Sun emission is also indicated (dotted line) (after Moutot and Boischot, 1961).
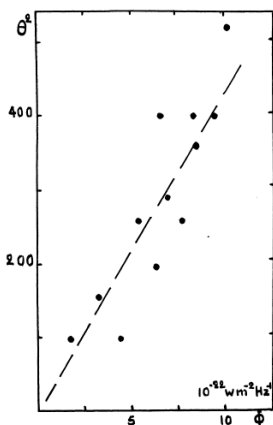

Figure 24: Plot of flux density (ϕ) versus the square of the apparent diameter (θ^2) for active centres at 169 MHz (after Moutot and Boischot, 1961).

Similar studies performed at 7.5 cm, 9.1 cm and 21 cm showed that, at decimetre wavelengths, these two families can no longer be distinguished. Furthermore, Kakinuma and Swarup (1962) showed that in general the flux density of strong radio sources is higher at the longer wavelengths than at 3 cm. Thus, Avignon et al. (1966) suggested that for the radio-emitting sources belonging to the first family, the spectrum between 3 cm and 6 cm could be flatter than for those belonging to the second family. They anticipated that this property could be of interest for forecasting solar flare activity.

3.3.2 The Slowly Varying Component at 169 MHz

3.2.2.1 *Observed Characteristics*

As already discussed in Section 3.2.2, Boischot (1958) showed that the shape of the Sun at 169 MHz varied from day to day. This is illustrated in Figure 23 for four successive days. Moutot and Boischot (1961) estimated that the apparent diameter of the radio sources superimposed on the quiet Sun ranged between 10′ and 20′. These sources could reach 15-20% of the flux of the quiet Sun. Moreover, they found a positive correlation between the square of the apparent diameters and the flux densities of these centres, as shown in Figure 24, and they concluded that the brightness temperature was approximately the same for all centres, and was $\sim 1.2 \times 10^6 \pm 10\%$ K.

In Figure 23, the maximum of emission attributed to the SVC follows the solar rotation and the authors assumed that the emission was associated with an active centre. However, in other cases, as shown in Figure 15 (left panel), the maximum did not rotate regularly, so the authors suggested that these cases corresponded to the presence of several active centres whose emissions were superimposed upon one another.

When they could distinguish the contribution of an emitting centre near the central meridian over a period of at least two days, they discussed the possibility of deducing the altitude of the emitting centre from its apparent velocity of rotation and its heliographic latitude. Assuming a mean latitude, L, of 20° for the

1958-1960 period, the mean altitude found during this interval was $h = 140{,}000$ km $\pm$ 30,000 km. A similar value of 125,000 km was found by Leblanc (1970), who extended this study to a larger number of observations during the period 1957-1968.

On four different occasions during 1959 the N-S Interferometer was used by Moutot and Boischot (1961) to determine the heliocentric latitude of active regions, and it was then possible to compute h for each of these with a much better accuracy. The values reported in Table 2 show some variation from one centre to another.

Moreover, Moutot and Boischot (ibid.) underlined that an important characteristic of these emissions was their directivity; no emissive region was observed at a distance $>10'$ from the central meridian of the Sun. This suggested that the directivity of the SVC at 169 MHz could be explained by assuming that the emissive regions were situated near the critical plasma level. In all cases, for sources located near the critical level refraction is important, so the emergent radiation is almost radial, whatever the initial direction. Consequently, the radiation emitted near the centre of the Sun will be received at the Earth, whereas for regions situated near the limb, the brightness temperature will be small.

3.3.2.2 *The Link with Optical Features: A Long History*

The SVC at metre wavelengths had been observed for decades, but its origin and its link with optical features was somewhat controversial. In Boischot (1958) and Moutot and Boischot (1961), the radio flux increases (RFI's) of the SVC were measured at 169 MHz with the E-W Interferometer, and were interpreted as the radio counterpart of the coronal enhancements which overlie calcium plages. As the radio sources often had large apparent diameters, of $>8'$, and could persist for several solar rotations, Leblanc (1970) proposed that RFI's would correspond to old and broadly-dispersed plages.

Subsequently, Axisa et al. (1971), using the same radio telescope, compared the radio sources at 169 MHz with the optical features, plages and filaments observed in Hα. They emphasized that

> When followed on photographs taken in Hα, the filaments are seen to suffer temporal changes in visibility, not apparent on the synoptic maps. (ibid.).

Thus they used for this comparison the synoptic maps from Meudon Observatory, where calcium plages and filaments were sketched (see Figure 25). On these maps, all the filaments were reported in Carrington co-ordinates at the dates of their heliographic central meridian passage, if they were visible for at least two days (whatever their helio-

Table 2: Calculated heights of four different active regions (after Moutot and Boischot, 1961: 175).

Date	h (km)
5-6 March 1959	200,000 ± 20,000
8-9 July 1959	240,000 ± 20,000
10-11 July 1959	80,000 ± 8,000
26-27 July 1959	190,000 ± 20,000

graphic longitude) during their transit of the solar disk. These synoptic charts allowed Axisa et al. (ibid.) to interpolate the position of the filaments on dates when they were not visible in the daily observations. They found that ~60% of the sources could be associated with one or several filaments and 5% with calcium plages; for 35% of them, the association either with calcium plages or with filaments was possible and thus inconclusive. For the RFI's correlated with filaments, the authors concluded that their emission originated in regions located at the base of streamers which overlay filaments. In addition, the correlation was extended to the direction of the filament: when a RFI was related to a filament (or a system of them) which extended over several tens of degrees perpendicular to the meridian, this RFI had the shape of a broad hump which remained at the meridian for several days; conversely, when the RFI corresponded to a short filament approximately parallel to the meridian, its rotation was more regular and the hump was narrower. As filaments traced the inversion line between two regions of opposite magnetic polarity, all of the RFI's correlated with filaments were representative of the same basic magnetic structure. This remark led to a coherent explanation of the radio sources whose shape would no longer be circular, but rather would have the form of elongated structures, called 'dense sheets', which would more or less follow the orientation of the underlying filaments, i.e. of the photospheric inversion line of magnetic polarity.
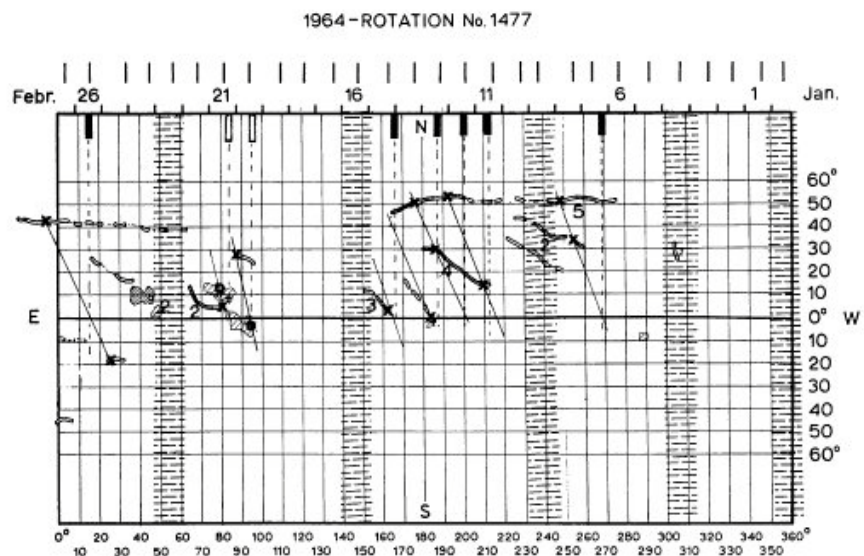

Figure 25: The association between RFI's (radio flux increases) and optical features. Black rectangles below the time scale of the synoptic map of Meudon Observatory indicate the meridian passage of a RFI related to filaments. Open rectangles correspond to the meridian passage of a RFI related to both filaments and calcium plages (undetermined cases). Dashed areas correspond to no available data. Crosses and heavy dots represent respectively the crossings of filaments and plages by the meridian trace (sketched by the light line) (after Axisa et al., 1971).
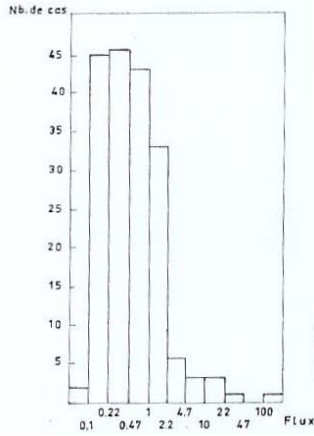
Figure 26: Histogram of flux densities (10^{-22} Wm^{-2}Hz^{-1}) of all centres (slowly varying component and storm centres) at 408 MHz (after Clavelier, 1967).

More than one decade later, when the Nançay Radioheliograph (NRH) observations became available, this radio telescope was employed as an aperture synthesis instrument using Earth rotation to obtain two-dimensional maps of the Sun at 169 MHz. The first observations showed no apparent association either with active regions or with filaments (Alissandrakis et al., 1985). Most of the sources appeared to be associated with inversion lines of photospheric magnetic polarity; they were located within the coronal plasma sheet, which delineates the inversion line between the north and south polarities of the large-scale magnetic field. Lantos and Alissandrakis (1996) proposed that the radio emission of the SVC came from arcades of moderately-dense loops spanning the neutral lines and located below the coronal streamer belt.

Quite recently, Mercier and Chambe obtained high-resolution maps of the SVC with the NRH at several frequencies. At 169 MHz, these maps show that many SVC sources appear as elongated bright ribbons oriented along the magnetic inversion lines of the photospheric field (to be published; private communication). These results are consistent with and indeed extend the early results from one-dimensional observations.
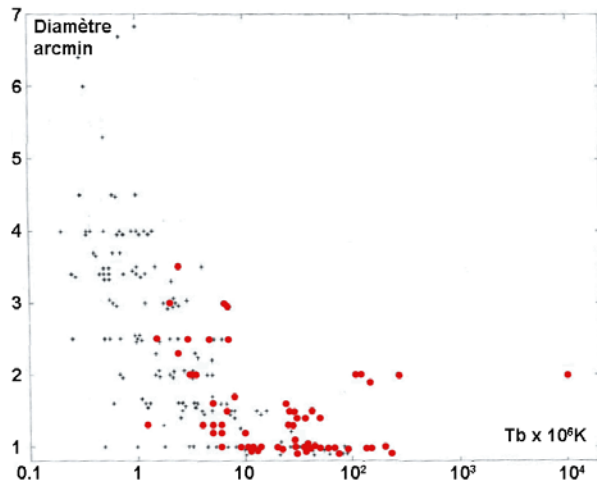

Figure 27: Plot of diameters versus brightness temperatures for all centres (slowly varying component and storm centres) observed at 408 MHz. The red circles indicate centres which were also observed at 169 MHz (after Clavelier, 1967).

3.3.3 408 MHz: Differentiation Between the SVC and Noise Storm Centres

Most of the results obtained at 408 MHz were published by Clavelier (1967; 1968a). The radio spectra displayed in Figure 18 show that the SVC and noise storm flux densities at 408 MHz in many cases are of the same order. The histogram of flux densities of all SVC and noise storm centres is shown in Figure 26. In about 90% of cases, the flux densities are $<2 \times 10^{-22}$ Wm^{-2}Hz^{-1}. Figure 27 shows the distribution of the centres as a function of their diameter and of their brightness temperature (T_b). Those centres which were
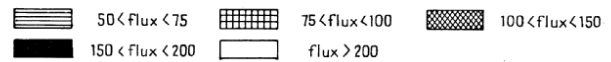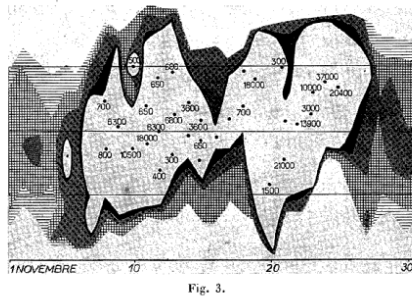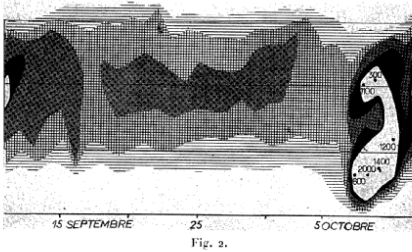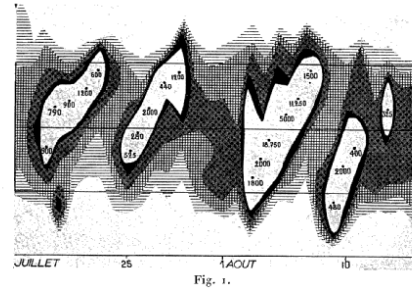

Figure 28: Three diagrams showing the distribution of solar radio emission at 169 MHz during the period July-November 1956. The horizontal lines represent the western limb, equator and eastern limb of the optical Sun. The active centres are indicated by dots, accompanied by their flux levels. The flux unit shown in the isophotes is 10^{-24} Wm^{-2}Hz^{-1} (after Avignon et al, 1957).

observed simultaneously at 169 MHz are indicated by red circles, and it is seen that centres with a high brightness temperature have in general a small diameter ($<2'$) and are associated with noise storms at 169 MHz. Conversely, centres with diameters of $>2.5'$ and $T_b < 5 \times 10^6$ K are not associated with noise storms. They are the sources of the SVC and are associated with faculae devoid of sunspots (Clavelier, 1968a).

3.4 Noise Storm Centres at 169 MHz and 408 MHz

At 169 and 408 MHz, noise storm emissions are the most frequent form of solar radio activity. They consist of a background continuum with superimposed

bursts of short duration (a fraction of a second), named by Wild and McCready (1950) Type I bursts (cf. Denisse, 1959a). The first systematic study of the continuum was carried out at Nançay with the large E-W Array at 169 MHz and later at 408 MHz.

3.4.1 169 MHz Emission

From 29 May 1956, daily solar observations were made with the E-W Interferometer. The first results on the diameter, duration, altitude and formation circumstances of the active centres at 169 MHz were published by Avignon et al., (1957; 1959) and Boischot (1958).

The basis for illustrating some of these parameters was a diagram that the French radio astronomers developed to show the daily distribution and intensity of individual active regions. Three examples of these diagrams are shown in Figure 28. In the first and third panels the Sun was particularly active, but in the middle panel it was relatively quiet. When the Sun is particularly active, a number of different centres may be present at the same time.

From these diagrams, the authors concluded that the flux densities of storm centres can reach 50 or 100 times those of the quiet Sun level. Most storm centres have diameters ranging between 3′ and 9′ (see Figure 29), but several of them are unresolved by the instrument and therefore could be <1′.
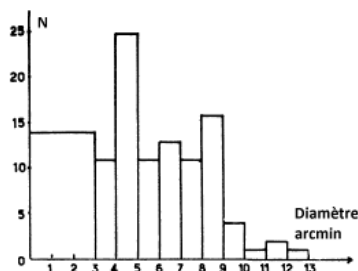

Figure 29: Histogram of the diameters of active centres, in minutes of arc (after Boischot, 1958).

The duration of these storm centres was very variable, from hours to days, but was always <6 days. Boischot (1958) noted that surely it was not limited by a beaming effect as one can observe these centres as far as 10′ beyond the optical limb of the Sun. When active centres could be associated with specific sunspots, it was possible to estimate the altitude of the centres above the photosphere using two methods: (1) by measuring their apparent speed of rotation and (2) by determining the points of appearance and disappearance of centres at the limb of the Sun. The results from both methods showed that the altitudes lay between 0.15 $R_\odot$ and 1 $R_\odot$, in general much higher than the critical altitude calculated for the normal corona at the observing frequency. Boischot (ibid.) and Blum and Malinge (1960) found that noise storm centres were not always located vertically above their associated sunspots, and that they sometimes did not follow the rotation of the optical Sun.

E-W and N-S positional determinations of storm centres by Blum and Malinge (1960) and Le Squeren (1963) resulted in quite precise identifications with optical centres, and the accuracy of the measurements was ~1′ in right ascension and 2-3′ in declination. But, in agreement with the one-dimensional (E-W) measure-
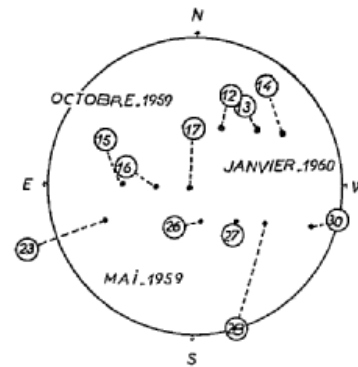

Figure 30: Solar map showing three different groups of positions of active centres (numbered circles) and their associated sunspots (black dots) on several successive days. The fact that the active centres do not always lie radially above their 'parent' sunspots is very apparent (after Blum and Malinge, 1960).

ments, there still appeared to be no geometrical relationship between the radio and optical centres. When a storm centre was visible during several consecutive days, its position relative to the associated optical centre did not remain fixed. This is illustrated in Figure 30, which shows the positions of three groups of noise storm centres relative to their associated sunspots. Blum and Malinge (1960: 3120; our translation) suggested that:

> Perhaps these displacements indicate actual motions of the noise storm centres in the corona, changes in altitude for example, but one can also interpret them as apparent displacements due to the propagation of radio waves in a coronal environment with structural irregularity.

Le Squeren (1963) determined the average position of a large number of centres. Figure 31 shows that, except at higher longitudes, the average storm centre was not radially-situated with respect to the leading spot of the associated sunspot group. This figure also indicates a systematic pole-ward displacement of the storm centres with respect to the spot groups. Consequently, Le Squeren emphasized that the determination of the altitudes of the centres was impossible, except for those cases that were located at high longitudes.

Using the two dimensional Nançay measurements of positions of noise storm centres at 169 MHz and 200 MHz polarization measurements made at Nera Observatory (Netherlands), Maligne (1960) investigated the sense of polarization of the continuum as a function of the latitude of the associated optical centre. Figure 32 shows clearly that there was a prevailing sense of polarization for each hemisphere. About 10% of the cen-
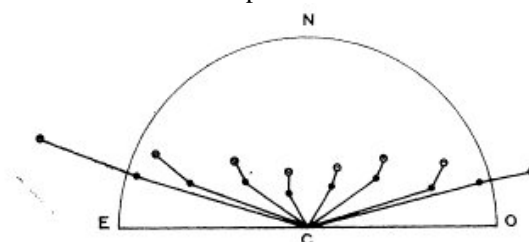

Figure 31: Mean positions of the noise storm centres (upper circles) and of their associated sunspots (lower circles) as the latter vary in heliocentric longitude. This figure shows a systematic displacement towards the central meridian of the Sun (after Le Squeren, 1963).
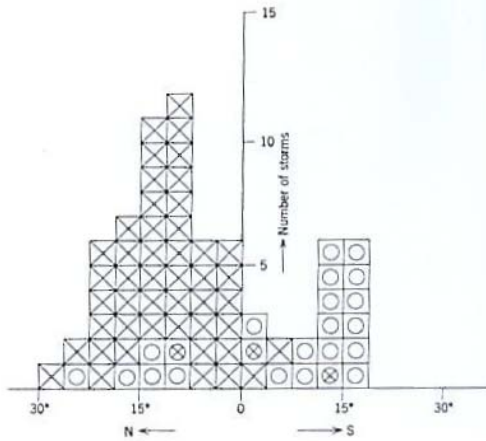
Figure 32: Latitude distribution of polarized storms. Key: circles = right-handed polarization; squares with crosses = left-handed polarization; circles with crosses = mixed polarization (after Le Squeren, 1963).

tres which were exceptions to the rule were associated with optical centres of rather complex structure, in which the magnetic field of the following spot was sometimes greater than that of the leading spot. Le Squeren (1963) proposed to associate the sense of polarization with the direction of the magnetic field in the leading spots, which was in agreement with the earlier results of Payne-Scott and Little (1951) and Komesaroff (1958). It was known that this direction was the same for all the optical centres in the same hemisphere. Thus it was concluded that the noise storm continua are usually polarized in the ordinary mode.
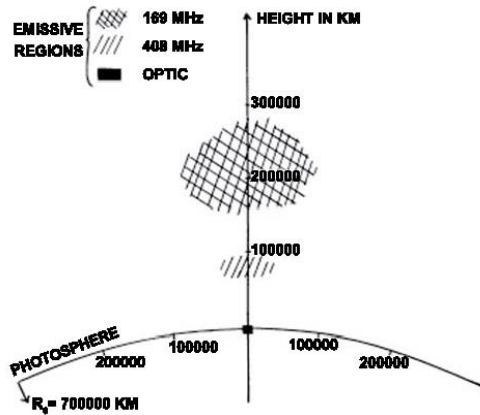

Figure 33: Schematic structure of a simple noise storm centre at 169 MHz and 408 MHz above an active region (after Clavelier, 1968).
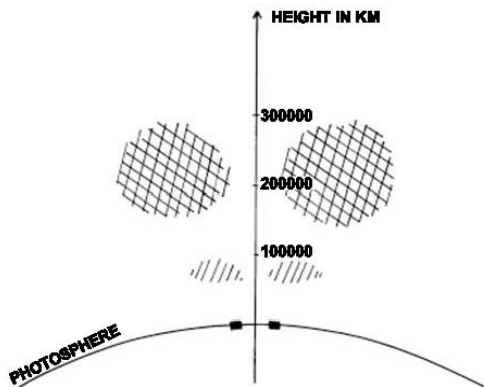

Figure 34: Schematic structure of a double noise storm centre at 169 MHz and 408 MHz (after Clavelier, 1968).

3.4.2 408 MHz Emission

Observations were obtained with a resolving power of 1.7′ which allowed the measurement of the E-W dimension of sources >1′ (Clavelier, 1967). The position of an emitting source was determined with an accuracy of 20″. The activity was compared with corresponding activities at 169 MHz and 9300 MHz, and it was concluded that the centres at 408 MHz were more stable that those at 169 MHz but less stable than centres at 9300 MHz. The respective characteristics of SVC and storm centres were summarized in Section 3.3.

Clavelier (1967) examined the association of noise storm centres with 'active regions' (AR's). Following the classification of the AR's by Martres et al. (1966), he showed that the quasi-totality of these centres was associated with magnetically-complex or anomalous eruptive AR's with anomalous inclination (i.e. an inversion line of polarities having a great inclination at the meridian).

Moreover, on certain days, Clavelier noted the existence of multiple (usually double) centres associated with the same active region (see Figure 6). The interesting result was that for all these double centres at 408 MHz, the corresponding AR appeared as two distinct eruptive zones with spots, each associated with a radio component (Clavelier, 1967; 1968a). The average height was accurately determined, and ranged between 70,000 and 80,000 km. Unfortunately, no polarization measurement was made at that time.

Results obtained at 169 and 408 MHz allowed Clavelier to draw a schematic picture of the structure of the active zones, as represented in Figures 33 and 34. The diameter was found to increase with altitude, but nothing could be said about the extension in latitude. Clavelier emphasized that the radio components of a double centre were probably independent. This was also confirmed by a study of the comparative evolution of head and tail fluxes in the same double centres: no correlation was found between the fluxes of these two components.

3.5 The Type IV Burst

3.5.1 The Discovery

In 1957 Boischot used the Nançay 32-element interferometer operating at 169 MHz to identify a new class of emission, the Type IV burst (Boischot 1957; 1958; 1959a). The observations revealed that a Type IV burst occurs after a solar flare, usually follows a Type II burst (whose emission is produced by large-scale shocks moving outwards through the corona) and lasts for tens of minutes. Type IV burst sources were generally of large diameter (typically 8′ to 12′) with no spatial structure (smooth appearance) and they moved outwards with speeds of several hundred km/s or more. An example is shown in Figure 35. Boischot and Denisse (1957) interpreted the Type IV emission as synchrotron radiation of relativistic electrons spiraling in the coronal magnetic field.

It was, however, rapidly recognized that Type IV bursts were much more complex events: they extended over a large range of frequencies in which several components with distinct physical origins could be distinguished. Intense centimetre-wave outbursts were found to be associated with metric Type IV emissions

(Avignon and Pick, 1959; Kundu, 1959). In 1961, two phases were distinguished by Pick-Gutmann (1961), as illustrated in Figure 36. The first phase (called 'flare-continuum' in 1970 by Wild) corresponded to a broad band emission, from centimetre to metre wavelengths, which started near the flash phase of the optical flare. The intensity variations were approximately similar at all frequencies and the radiation had little directivity. The second phase, called 'continuum storm' (or 'stationary Type IV burst' in 1963 by Wild et al.) was characterized by a smooth continuum detected from decimetre to decametre wavelengths which could last many hours and transformed progressively into an ordinary Type I storm. The emitting source was stationary, had a small angular diameter, was strongly polarized in the ordinary mode and was directed. Taking into consideration all of these properties, the continuum storm was interpreted as due to Cerenkov plasma radiation.

3.5.2 Association between Radio Emission and Energetic Particles Detected at the Sun or in the Vicinity of the Earth

3.5.2.1 *Association between Type IV Bursts and High Energy Proton Events*

The fact that Type IV emissions reveal the presence in the corona of MeV electrons stimulated many investigations on the association of these outstanding solar events with energetic particles detected in the environment of the Earth. Avignon and Pick-Gutmann (1959), and Pick-Gutmann (1961) investigated the association between Type IV bursts with relativistic protons detected by ground-level cosmic ray monitors, and proton events of lower maximum energy detected indirectly by their ionospheric effects: Polar Cap Absorptions (PCA's) produced by 10-100 MeV protons were discovered during the International Geophysical Year (IGY, 1957-1959) (see Hakura and Goh, 1959; Thompson and Maxwell, 1960). Avignon and Pick-Gutmann (1959) found a quasi-systematic association between proton events and Type IV bursts radiating in the microwave domain with flux densities greater than 10^{-17} W m^{-2} Hz^{-1} and followed by storm continuum at metre wavelengths. These events were more favourably located in the western solar hemisphere. Avignon and Pick-Gutmann (ibid.) defined the radio importance of a flare as the energy radiated at 10 cm (i.e. the flux density at the maximum multiplied by the duration).

3.5.2.2 *Optical Characteristics of Type IV Bursts Associated with Flares*

Avignon, Martres and Pick (1964) examined the characteristics of chromospheric flares that gave rise to Type IV bursts associated with PCA's. They found that for all the 16 selected events, except one, the active region and the flare were of a particular structure previously discovered by Ellison et al. (1962) in a study of flares connected with ground-level cosmic ray increases: two rows of centres with opposite polarities very close to each other, where the flare started between the two centres and evolved into two chains (so-called 'ribbon flares') that overlapped the spots (see Figure 37, Configuration A).

Building on an earlier study (see Martres and Pick, 1962), Avignon, Martres and Pick (1964) then considered the more general case of flares with long dur-
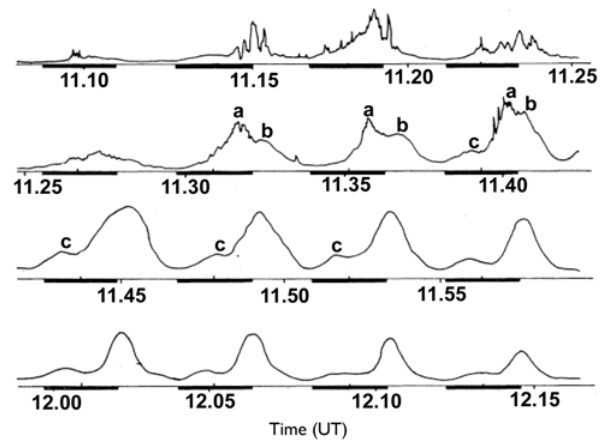

Figure 35: The Type IV burst of 7 November 1956 recorded at 169 MHz by the E-W Nançay interferometer array. This figure displays a succession of scans versus time. The variable source 'a' is probably the source of a Type II burst followed by the smooth source 'b' of the Type IV burst; the peaks 'c' are generated in the side lobes of the interferometer; the black bars indicate the position of the photospheric disk through the successive main lobes of the interferometer; the recording time of each main lobe is indicated below (after Boischot, 1958).
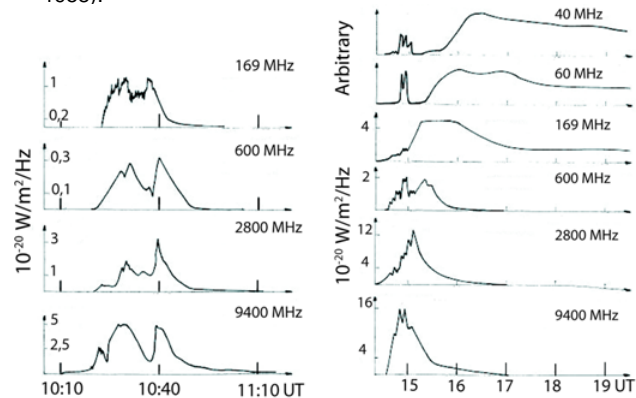

Figure 36 (left)*:* First phase of the Type IV burst on 28 August 1958, showing the flux evolution measured at several frequencies; and (right): Flux evolution of another Type IV burst observed on 22 August 1958, when the first phase seen from high frequencies to 169 MHz at least is followed by a continuum storm of long duration that is well developed below 600 MHz (adapted from Pick-Gutmann, 1961).
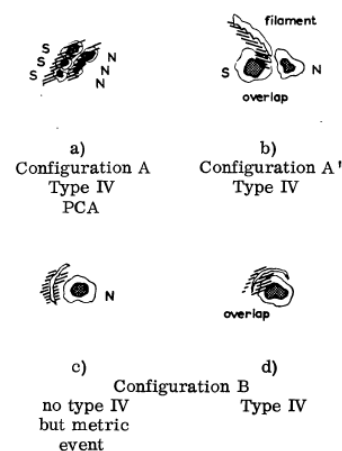

Figure 37: Characteristics of flares at optical wavelengths associated with long-duration radio events at metre wavelengths that are either Type IV bursts or noise-storm enhancements (adapted from Avignon, Martres and Pick, 1964).
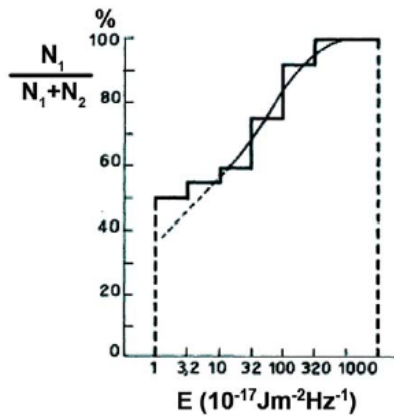
Figure 38: Probability of a flare to be associated with a SSC vs. their radio importance, i.e. the energy radiated at 2800 MHz. N1 and N2 correspond to the number of cases which are respectively geomagnetically-active or -inactive (after Caroubalos, 1964).

ation radio events at metre wavelengths which were either Type IV bursts or noise-storm enhancements. They were led to propose a new classification based on the radio importance and schematized in Figure 37.

For those events that were not associated with PCAs, the existence of a 'plage-filament', which occurred at the boundary between opposite polarities of the magnetic field, seemed to determine the location of the Hα flare and the occurrence of the metric event. When the configuration was A′ or B-c), and not B-d), the metre-wavelength Type IV event seemed to be associated with an Hα flare overlapping a sunspot. It was concluded that the occurrence of strong radio emission was enhanced by the presence of a strong gradient of the longitudinal magnetic field due to the proximity of spots of opposite polarities (see also Section 3.3 and Figure 21).

3.5.2.3 *Solar Radio Bursts and Geomagnetic Storms*

In 1964, Caroubalos investigated the association between Type IV bursts and sudden storm commencements (SSCs). Each Type IV burst was characterized by two parameters: its radio importance (the energy radiated at 10 cm) and its spectral character, defined as the ratio p of the duration of the metric emission measured at 169 MHz to the duration of the microwave emission measured at 10 cm (2800 MHz); the value of this parameter provides information on the existence of a second phase. The main results of this study are summarized as follows:
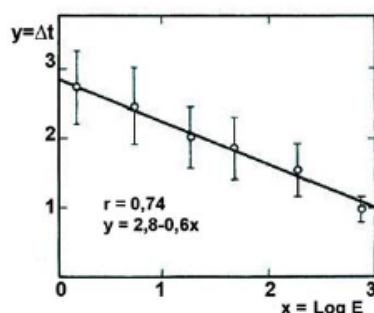

Figure 39: Time of disturbances followed by a SSC vs. the radio importance of the associated flare (after Caroubalos, 1964)

(1) The probability for Type IV bursts to be followed by SSCs is a function of their radio importance. Figure 38 shows that this probability increases rapidly for events with energies greater than 30×10^{-17} Jm^{-2} Hz^{-1} at 2800 MHz. The existence of a second phase of relatively long duration appears to be an essential condition for a Type IV burst to be followed by a SSC.

(2) There is a statistical relationship between the Sun-Earth transit time of the disturbances responsible for SSCs and the radio energy emitted by the associated Type IV bursts (see Figure 39).

In January 1960, a review paper on the properties of Type IV bursts and on their association with solar cosmic rays was presented at the First International Space Science Symposium in Nice (Denisse, et al., 1960).

4 THE CRAB NEBULA AND THE OUTER CORONA

With 3.8′ E-W pencil beams 2° apart, the 169 MHz E-W interferometer had the potential to also contribute in a significant way to the study of the outer corona through the observation of selected discrete radio sources while they were near the Sun.

The first such project took place in June 1957 when the Crab Nebula (Taurus A) was occulted by the Sun. Although observations were only possible on June 11 and 13, an increase in the diameter of the source was noted on both occasions. But more importantly, there was an

… actual *increase* of total flux received from the Crab Nebula on the 13th; this result suggests that refractive processes in the corona might play an important role. (Blum and Boischot, 1957: 206).

In June of 1958 the Crab Nebula was again used to investigate the outer corona, and the Nançay observations confirmed both the increase in source diameter and in flux density as Taurus A approached the Sun. Figure 40, where data from 1957 and 1958 have been pooled, shows that both effects commenced when the Crab Nebula was at about $15R_{\odot}$. In a previous paper in this series we noted (Orchiston et al, 2007: 239) that it is interesting to compare these French results with Slee's 85.5 MHz observations of the same 1957 and 1958 events. He found that

… the distribution of Crab nebula radiation is markedly affected by refraction and large-scale coronal irregularities. The secondary peak … was recorded in both 1957 and 1958, and suggests the existence of semi-permanent regions in the corona of higher than average electron density. (Slee, 1959: 151).

Slee also noted short-term changes in the transmission properties of the corona, which he associated with the ejection of disturbances from active regions on the solar disk.

5 NON-SOLAR RESEARCH WITH THE 169 MHz INTERFEROMETERS

5.1 The E-W Interferometer

As noted in a previous paper in this series (Orchiston et al., 2007: 239):

One of the most challenging problems facing radio astronomers in the 1940s and 50s was to identify optical correlates for the many discrete sources found in the

course of the various sky surveys. Because of the comparative lack of resolution at radio wavelengths, it was difficult to determine the precise positions of most sources, but instruments like the Nançay 32-element E-W grating array (with its 3.8′ pencil beams) offered some hope. It is no surprise, therefore, to learn that this instrument was used by Boischot (1959[b]) to investigate source positions in the late 1950s. He subsequently published a table containing 25 different sources between Declination +60° and −20°, listing for each the Right Ascension, Declination, diameter or an upper limit to this parameter, the flux density and any correlation that could be made with sources detected by previous investigators.

5.2 The N-S Interferometer

By the end of 1961 the N-S interferometer was operational, and its $3.4 \times 7'$ pencil beam was used extensively by Mohan Joshi (1962) at 169 MHz for non-solar work. His principal project was to measure the precise positions and flux densities of 112 different radio sources. Most of these were identified with discrete sources recorded earlier at Fleurs in Australia (Mills, Slee and Hill, 1958) or during the Cambridge 3C survey (Edge et al., 1959).

An important outcome of Joshi's work (1962) was to resolve the controversy surrounding the optical identification of the radio source Hercules A. In the relevant area of the sky there were three different galaxies, but sources recorded at the Owens Valley Radio Observatory and Cambridge tallied with two of these. Joshi's Nançay observations showed conclusively that the 'Cambridge galaxy' was the correct identification (see Figure 41).

6 HERITAGE ISSUES

In 2003, the IAU established the Historic Radio Astronomy Working Group under the joint umbrellas of Commissions 40 (Radio Astronomy) and 41 (History of Astronomy) in order to encourage research into the early history of radio astronomy. One of the objectives of the WG is to establish how many of the pioneering radio telescopes used worldwide prior to 1961 have survived, and France has an important 'claim to fame' in this regard.

One of the Nançay radio telescopes discussed in this paper—the distinctive 9300 MHz 16-element interferometer designed by Steinberg and Pick—has survived in close to its original configuration, apart from the replacement of valves by transistors in the receiving system. Actually, to say that this radio telescope "… has survived …" is something of an understatement, for after more than fifty years operation it continues to contribute to science by providing daily strip scans of the one-dimensional distribution of solar radio emission

As the founder and inaugural Chair of the IAU Working Group, one of the authors of this paper (W.O.) believes that from a heritage perspective the 9300 MHz grating array at Nançay stands as a beacon of hope for world radio astronomy. Since almost all of the notable antennas from the pre-1961 era have long since disappeared, this radio telescope is an important part of our *international* radio astronomical heritage, and as such it should be preserved for the benefit of future generations. Furthermore, in terms of hardware,
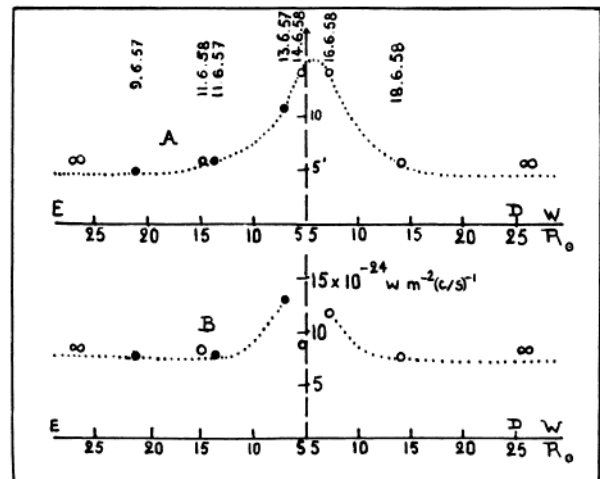

Figure 40: Variations in the apparent diameter (curve A) and flux density (curve B) of the Crab Nebula as it was occulted by the Sun in 1957 and 1958 (after Blum and Boischot, 1959: 283).

it is all that remains today from the pioneering era of French radio astronomy.

7 CONCLUDING REMARKS: NANÇAY AND THE FOUR LAST DECADES

The end of the 1960s was marked by the development in solar radio astronomy of a new generation of instruments giving access to spatially-resolved observations of the corona, with the construction of the first two radio-imaging instruments, the Culgoora Radioheliograph in Australia (Wild, 1967) and the Teepee T-Array at the Clark Lake Radio Observatory in the U.S.A. (Erickson and Fisher, 1971). In France, a new radio heliograph (NRH) was designed for Nançay which would provide images with a high temporal cadence of 100 images per second. This instrument was built in successive stages at the single frequency of 169 MHz. The first version, operational in 1976, was restricted to one dimension in the E-W direction (Bonmartin et al., 1977). Today, the NRH provides 2-D images in the frequency range 150-450 MHz. It allows quasi-simultaneous multi-frequency observations with a maximum number of 10 frequencies and a limit of 200 images per second (Kerdraon and Delouis, 1997).
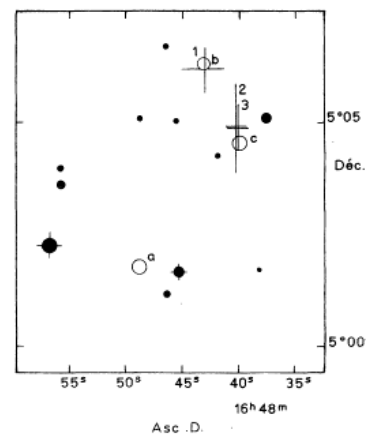

Figure 41: The region of the sky containing the discrete radio source Hercules A. Galaxies are marked by a, b and c and the crosses indicate source positions obtained by the Caltech (1), Cambridge (2) and Nançay (3) groups (after Joshi, 1962: 398).

In Nançay, there was also emphasis on high resolution spectroscopy at decametre wavelengths of solar and Jovian radio bursts, both in time and frequency (see Boischot, 1974). The Nançay Decameter Array operating in the 10-80 MHz frequency range was designed and built in the mid-1970s (Boischot et al., 1980; Lecacheux, 2000), and consists of two phased antenna arrays in opposite senses of circular polarization, each with an effective aperture of 4,000 m^2.

We do not intend to describe here the large number of results obtained in the last four decades with these instruments. We shall, however, emphasize the importance of coupling ground-based radio observations with space radio instruments for simultaneous or complementary observations in other parts of the electromagnetic spectrum (e.g. see Pick and Vilmer, 2008). The involvement of Nançay in space missions was first illustrated by the STEREO-1 (Caroubalos and Steinberg, 1974) and STEREO-5 (Poquerusse and Steinberg, 1978) experiments which were designed to detect and measure the directivity of solar burst radiation at 169 MHZ and at 60 and 30 MHz respectively. These experiments were based on simultaneous observations from the Earth (Nançay) and from a Soviet space probe (Mars-3 for STEREO-1 and Mars-7 for STEREO-5). Shortly afterwards, Nançay was officially associated with NASA's Voyager mission, a spare model of the flight radio astronomy instrument (PRA) being fed by the Nançay Decameter Array at the times of the Jupiter encounters (Boischot et al., 1981).

Since this period, the Nançay radio astronomers have offered regular significant contributions to many European, Russian and U.S. space experiments dedicated to the study of the solar corona, the Jovian magnetosphere and the heliosphere, including MARS 3 and 7, GRANAT, SMM, ULYSSES, Galileo, WIND, ACE, SOHO, STEREO and RHESSI.

8 NOTES

1. In 1952, these were merely three of the four radio astronomy field stations maintained by the Division of Radiophysics in and near Sydney. The fourth was located at Dover Heights. For a review of all of the field stations and remote sites established by the Division between 1946 and 1961 see Orchiston and Slee (2005). For a detailed account of the Dapto field station, which was devoted solely to solar research, see Stewart (2009) and Stewart et al. (2011). For details of the solar grating arrays at the Potts Hill field station see Wendt (2008), and Wendt et al. (2008; 2011).
2. For events leading up to the establishment of the Nançay field station see Orchiston et al. (2007: 225-226) and Steinberg (2004).
3. Radio astronomy is not just about science and instrumentation; it sometimes involves politics and public opinion. Steinberg (2001: 513) tells about an interesting episode concerning the railway line that was to be built at Nançay for the two Würzburg antennas:

> When the inhabitants of Nançay village heard through rumours that a rail-line was to be built in the radioastronomy station, they immediately inferred that the line was going to be linked to the National Railways network through several of their pieces of land and they became very worried. In November

1953, we thus organized a meeting of all Nançay inhabitants. I told the villagers what our plans were and insisted on the fact that our gauge was to be 6 m as compared to 1.44 m for the regular lines. We succeeded in reassuring them.

4. This project was initiated under the auspices of the IAU Working Group on Historic Radio Astronomy in 2006, and five papers have been published to date. The first dealt with Nordmann's attempt to detect solar radio emission in 1901 (Débarbat et al., 2007); the second with early solar eclipse observations (Orchiston and Steinberg, 2007); the third with the Würzburg antennas that were at Marcoussis, Meudon and Nançay (Orchiston et al., 2007); the fourth with early solar work conducted at the École Normale Supérieure, Marcoussis and Nançay (Orchiston et al., 2009); and the fifth with the Nançay Large Radio Telescope (Lequeux et al., 2010). For an earlier overview see Denisse (1984).

9 ACKNOWLEDGEMENTS

10 REFERENCES

Alissandrakis, C.-E., Lantos, P., and Nicolaidis, E., 1985. Coronal structures observed at metric wavelengths with the Nancay radioheliograph. *Solar Physics*, 97, 267-282.

Avignon, Y., and Lantos, P., 1971. Emission thermique de la couronne calme sur 169 MHz au cours du cycle solaire. *Comptes Rendus de l'Académie des Sciences*, 273, 684-685.

Avignon, Y., and Le Squeren-Malinge, A.-M., 1961. Dimensions du Soleil calme sur 169 MHz. *Comptes Rendus de l'Académie des Sciences*, 253, 2859-2861.

Avignon, Y., and Pick, M., 1959. Relation entre les émissions de type IV et d'autres formes d'activité solaire. *Comptes Rendus de l'Académie des Sciences*, 248, 368-371.

Avignon, Y., and Pick-Gutmann, M., 1959. Relation entre les émissions solaires de rayons cosmiques et les sursauts de type IV. *Comptes Rendus de l'Académie des Sciences*, 249, 2276-2278.

Avignon, Y., Boischot, A., and Simon, P., 1959. Observation interférométrique à 169 mc/s des centres R, sources des orages de bruit. In Bracewell, 240-244.

Avignon, Y., Martres, M.J., and Pick, M., 1964. Identification de classes d'éruptions chromosphériques associées aux émissions de rayons cosmiques et à l'activité radioélectrique. *Annales d'Astrophysique*, 27, 23-28.

Avignon, Y., Martres, M.-J., and Pick, M., 1966. Étude de la 'composante lentement variable' en relation avec la structure des centres d'activité solaire associés. *Annales d'Astrophysique*, 29, 33-42.

Avignon, Y., Lantos, P., Palagi, F., and Patriarchi, P., 1975. The quiet Sun brightness temperature at 408 MHz. *Solar Physics*, 45, 141-145.

Avignon, Y., Blum, É.J., Boischot, A., Charvin, R., Ginat, M., and Simon, P., 1957. Observation des orages radio-électriques solaires avec le grand interféromètre de Nançay. *Comptes Rendus de l'Académie des Sciences*, 244, 1460-1463.

Axisa, F., Avignon, Y., Martres, M.-J., Pick, M., and Simon, P., 1971. Solar coronal streamers observed at 169 MHz with the Nançay East-West Radioheliograph. *Solar Physics*, 19, 110-127.

Benoit G., 1956. Diplôme d'Études Supérieures. Paris.

Blum, É.J., 1961. Le réseau nord-sud a lobes multiples. Complément au grand Interféromètre de la Station de Nançay. *Annales d'Astrophysique*, 24, 359-366.

Blum, E.J., and Boischot, A., 1957. Occultation of the Crab Nebula by the solar corona. *The Observatory*, 77, 205-206.

Blum, É.-J., and Malinge, A.-M., 1960. Étude des positions relatives des sources d'orage radioélectrique solaire et des centres d'activité optique associés. *Comptes Rendus de l'Académie des Sciences*, 250, 3119-3121.

Blum, É.J., Boischot, A., and Ginat, M., 1956. L'interféromètre à antennes multiples de la Station de Nançay. *Comptes Rendus de l'Académie des Sciences*, 243, 19-22.

Blum, É.J., Boischot, A., and Ginat, M., 1957. Le grand interféromètre de Nançay. *Annales d'Astrophysique*, 20, 155-164.

Boischot, A., 1957. Caractères d'un type d'émission hertzienne associé à certaines éruptions chromosphériques. *Comptes Rendus de l'Académie des Sciences*, 244, 1326-1329.

Boischot, A., 1958. Étude du rayonnement radioélectrique solaires sur 169 MHz, a l'aide d'un grand interféromètre a réseau. *Annales d'Astrophysique*, 21, 273-344.

Boischot, A., 1959a. Les emissions de Type IV. In Bracewell, 186-187.

Boischot, A., 1959b. Résultats préliminaires de l'observation des radiosources à l'aide de l'interféromètre de Nançay. In Bracewell, 492-495.

Boischot, A., 1974. Radioastronomy on decameter wavelengths at Meudon and Nançay Observatories. *Solar Physics*, 36, 517-522.

Boischot, A., and Denisse, J.-F., 1957. Les émissions de type IV et l'origine des rayons cosmiques associé aux éruptions chromosphériques. *Comptes Rendus de l'Académie des Sciences*, 245, 2194-2197.

Boischot, A., and Simon, P., 1959. La composante lentement variable du rayonnement solaire sur 169 mc/s. In Bracewell, 140-142.

Boischot, A., Lecacheux, A., Kaiser, M.L., Desch, M.D., Alexander, J.K., and Warwick, J.W., 1981. Radio Jupiter after Voyager: an overview of the Planetary Radio Astronomy observations. *Journal of Geophysical Research*, 86, 8213-8226.

Bonmartin, J., Jones, I., Kerdraon, A., Lacombe, A., Lantos, M.F., Lantos, P., Mercier, C., Pick, M., Trottet, G., and Bruley, M., 1977. The Mark II Nançay Radioheliograph. *Solar Physics*, 55, 251-261.

Bracewell, R.N. (ed.), 1959. *Paris Symposium on Radio Astronomy...* Stanford, Stanford University Press.

Caroubalos, C., 1964. Contribution à l'étude de l'activité sol-

aire en relation avec ses effects géophysiques. *Annales d'Astrophysique*, 27, 333-388.

Caroubalos, C., and Martres M.-J., 1964. Une propriété morphologique des groups de taches solaires responsables des éruptions accompagnées d'émissions en ondes métriques. *Comptes Rendus de l'Académie des Sciences*, 258, 830-832.

Caroubalos, C., and Steinberg, J.-L., 1974. Evidence of solar burst directivity at 169 MHz from simultaneous ground based and deep space observations (STEREO-1 Preliminary Results). *Annales d'Astrophysique*, 32, 245-253.

Christiansen, W.N., and Mathewson, D.S., 1959. The origin of the slowly varying component. In Bracewell, 108-117.

Christiansen, W.N., and Warburton, J.A., 1953. The distribution of radio brightness over the solar disk at a wavelength of 21 cm. Part II - The quiet Sun - one dimensional observations. *Australian Journal of Physics*, 6, 262-271.

Clavelier, B., 1966. Mise en service d'un nouveau réseau Est-Ouest sur 408 MHz à haut pouvoir de résolution destiné a l'étude du Soleil. *Comptes Rendus de l'Académie des Sciences*, 262, 225-228.

Clavelier, B., 1967. Etude de l'activité solaire à 408 MHz. *Annales d'Astrophysique*, 30, 895-924.

Clavelier, B. 1968a. Some results of solar activity at 408 MHz.. In Kiepenheuer, Karl Otto (ed.). *Structure and Development of Solar Active Regions*. Dordrecht, Reidel (International Astronomical Union Symposium No. 35). Pp. 556-564.

Clavelier, B., 1968b. Un réseau pour l'étude des structures de l'activité solaire sur 408 MHz: description de l'appareil et premiers résultats. *Journal des Observateurs*, 51, 99-121.

Conway, R.G., and O'Brien, P.A., 1956. The distribution of brightness at metre wave-lengths across the solar disk. *Monthly Notices of the Royal Astronomical Society*, 116, 386-394.

Chiuderi-Drago, F., Avignon, Y., and Thomas, R.J., 1977. Structure of coronal holes from UV and radio observations. *Solar Physics*, 51, 143-158.

Débarbat, S., Lequeux, J., and Orchiston, W., 2007. Highlighting the history of French radio astronomy. 1: Nordmann's attempt to detect solar radio emission in 1901. *Journal of Astronomical History and Heritage*, 10, 3-10.

Denisse, J.F., 1959a. Les sources d'émissions radioelectriques du Soleil. In Bracewell, 81-88.

Denisse, J.F., 1959b. Relation entre les emissions de rayons cosmiques solaires et certains sursauts radioelectriques. In Bracewell, 237-239.

Denisse, J.F., 1984. The early years of radio astronomy in France. In Sullivan, 303-315.

Denisse, J.-F., Boischot, A., and Pick-Gutmann, M., 1960. Propriértés des éruptions chromosphériques associées à la production de rayons cosmiques par le Soleil. In *Space Research. Proceedings of the First Space Science Symposium (Nice, 11-16, 1960)*. Amsterdam, North Holland Publishing. Pp. 637-648.

Dulk, G.A., and Sheridan, K.V., 1974. The structure of the middle corona from observations at 80 and 160 MHz. *Solar Physics*, 36, 191-202.

Dulk, G.A., Sheridan, K.V., Smerd, S.F., and Withbroe, G.L.,1977. Radio and EUV observations of a coronal hole. *Solar Physics*, 52, 349-367.

Edge, D.O., Shakeshaft, J.R., McAdam, W.B., Baldwin, J.E., and Archer, S., 1959. A survey of radio sources at a frequency of 178 Mc/s. *Memoirs of the Royal Astronomical Society*, 68, 37-60.

Ellison, M.A., McKenna, S.M.P., and Reid, J.H., 1962. Cosmic ray flares associated with the 1961 July event. *Monthly Notices of the Royal Astronomical Society*, 124, 263-274.

Erickson, W.C., and Fisher, J.R., 1971. The new fully steerable decametric array at Clark Lake. *Bulletin of the American Astronomical Society*, 3, 243.

Gutmann, M., and Steinberg, J.-L., 1959. Résultats préliminaires obtenus avec l'interféromètre à 8 antennes sur 3 cm de longueur d'onde. In Bracewell, 123-124.

Hakura, Y., and Goh, T.J., 1959. Pre-sc polar cap ionospheric blackout and Type IV solar radio outburst. *Radio Research Laboratory [of Japan]*, 6, 635-650.

Joshi, M., 1962. Mesures précises de position des radiosources à 169 MHz. *Annales d'Astrophysique*, 25, 377-399.

Kakinuma, T., and Swarup, G., 1962. A model for the sources of the slowly varying component of microwave solar radiation. *Astrophysical Journal*, 136, 975-994.

Kerdraon, A., and Delouis, J.-M., 1997. The Nançay Radioheliograph. In Trottet, G. (ed.). *Coronal Physics from Radio and Space Observations*. Dordrecht, Springer. Pp. 192-201.

Komesaroff, M., 1958. Polarization measurements of the three spectral types of solar radio bursts. *Australian Journal of Physics*, 11, 201-214.

Kundu, M.R., 1959. Structures et propriétés des sources d'activité solaire sur ondes centimétriques. *Annales d'Astrophysique*, 22, 1-100.

Lantos, P., and Alissandrakis, C.E., 1996. Coronal sources at meter and optical wavelengths during the declining phase of the solar cycle. *Solar Physics*, 165, 83-98.

Lantos, P., and Avignon, Y., 1975. The metric quiet Sun during two cycles of activity and the nature of the coronal holes. *Astronomy and Astrophysics*, 41, 137-142.

Leblanc, Y., 1970. Coronal enhancements. *Annales d'Astrophysique*, 4, 315-330.

Leblanc, Y., and Le Squeren, A.M., 1969. Dimensions, temperature and electron density of the quiet corona. *Astronomy and Astrophysics*, 1, 239-248.

Lecacheux, A., 2000. The Nançay Decameter Array: a useful step towards giant, new generation radio telescopes for long wavelength radio astronomy. In Stone, R.G., Weiler, K.W., Goldstein, M.L., and Bougerot, J.-L. (eds.). *Radio Astronomy at Long Wavelengths*. Washington, American Geophysical Union (Geophysical Monograph Series, Volume 119. Pp. 321-328.

Lequeux, J., Steinberg, J.-L., and Orchiston, W., 2010. Highlighting the history of French radio astronomy. 5: The Nançay Large Radio Telescope. *Journal of Astronomical History and Heritage*, 13, 29-42.

Le Squeren, A.-M., 1963. Étude des orages radioélectriques solaires sur 169 MHz a l'aide de l'interféromètre en croix de la station de Nançay. *Annales d'Astrophysique*, 26, 97-152.

Liu Xu Zhao, and He Xiang Tao, 1974.Observations of solar radio emissions at 146 MHz. Instrumental and data analysis. *Acta Astronomica Sinica*, 15, 61-72.

Malinge, A.-M., 1960. Relation entre la position et le sens de polarisation des orages radioélectriques solaires. *Comptes Rendus de l'Académie des Sciences*, 250, 1186-1188.

Malinge, A.-M., Blum, É.-J., Ginat, M., and Parise, M., 1959. La branche nord-sud du Grand Interféromètre de la station de Nançay. *Comptes Rendus de l'Académie des Sciences*, 249, 2009-2011.

Martres, M.-J., and Pick, M., 1962. Caractères propres aux éruptions chromosphériques associées a des émissions radioélectriques. *Annales d'Astrophysique*, 25, 293-300.

Martres, M.-J., Michard, R., and Soru-Iscovici, I., 1966. Étude morphologique de la structure magnétique des régions actives en relation avec les phénomènes chromosphériques et les éruptions solaires. Classification magnétique et éruptivité. *Annales d'Astrophysique*, 29, 245-248.

Mills, B.Y., Slee, O.B., and Hill, E.R., 1958. A catalogue of radio sources between declinations +10° and −20°. *Australian Journal of Physics*, 11, 360-387.

Moutot, M., and Boischot, A., 1961. Étude du rayonnement thermique des centres d'activité solaire sur 169 MHz. *Annales d'Astrophysique*, 24, 171-179.

Orchiston, W. and Slee, B. 2005. The Radiophysics field stations and the early development of radio astronomy. In Orchiston, W. (ed.). *The New Astronomy: Opening the Electromagnetic Window and Expanding our View of Planet Earth*. Dordrecht, Springer. Pp. 119-168.

Orchiston, W., and Steinberg, J.-L., 2007. Highlighting the history of French radio astronomy. 2: The solar eclipse observations of 1949-1954. *Journal of Astronomical History and Heritage*, 10, 11-19.

Orchiston, W., Lequeux, J., Steinberg, J.-L., and Delannoy, J., 2007. Highlighting the history of French radio astronomy. 3: The Würzburg antennas at Marcoussis, Meudon and Nançay. *Journal of Astronomical History and Heritage*, 10, 221-245.

Orchiston, W., Steinberg, J.-L., Kundu, M., Arsac, J., Blum, E.-J., and Boischot, A., 2009. Highlighting the history of French radio astronomy. 4: Early solar research at the École Normale Supérieure, Marcoussis and Nançay. *Journal of Astronomical History and Heritage*, 12, 175-188.

Payne-Scott, R., and Little, A.G., 1951. The position and movement on the solar disk of sources of radiation at a frequency of 97 Mc/s. II. Noise storms. *Australian Journal of Scientific Research*, 4, 508-525.

Pick-Gutmann, M., 1961. Évolution des émissions radioélectriques solaires de Type IV et leur relation avec d'autres phénomènes solaires et géophysiques. *Annales d'Astrophysique*, 24, 183-210.

Pick-Gutmann, M., and Steinberg, J.-L., 1959. Réseau à 16 antennes fonctionnant sur 9300 MHz. *Comptes Rendus de l'Académie des Sciences*, 248, 2452-2454.

Pick, M., and Steinberg, J.-L., 1961. Réseau a seize antennes fonctionnant sur 9300 MHz a la station radioastronomique de Nançay. *Annales d'Astrophysique*, 24, 45-53.

Pick, M., and Vilmer, N., 2008. Sixty-five years of solar radio-astronomy: flares, coronal mass ejections and Sun-Earth connection. *Astronomy and Astrophysics Review*, 16, 1-153.

Poquérusse, M., and Steinberg, J.L., 1978. First results of the STEREO-5 experiment - evidence of ionospheric intensity scintillation of solar radio bursts at decameter wavelengths. *Astronomy and Astrophysics*, 65, L23-L26.

Slee, O.B., 1959. Occultations of the Crab Nebula by the solar corona in June 1957 and 1958. *Australian Journal of Physics*, 12, 134-156.

Steinberg, J.-L., 2001. The scientific career of a team leader. *Planetary and Space Science*, 49, 511-522.

Steinberg, J.-L., 2004. La création de la station de Nançay. *L'Astronomie*, 118, 626-631.

Stewart, R.T., 2009. The Contribution of the CSIRO Division of Radiophysics Penrith and Dapto Field Stations to International Radio Astronomy. Ph.D. Thesis, Centre for Astronomy, James Cook University (Townsville, Australia).

Stewart, R., Orchiston, W., and Slee, B., 2011. The contribution of the Division of Radiophysics Dapto field station to solar radio astronomy, 1942-1964. In Orchiston, W., Nakamura, T., and Strom, R. (eds.). *Highlighting the History of Astronomy in the Asia-Pacific Region*. New York, Springer. In press.

Sullivan, W.T. III (ed.), 1984. *The Early Years of Radio Astronomy: Reflections Fifty Years after Jansky*. Cambridge, Cambridge University Press.

Thompson, A.R., and Maxwell, A., 1960. Solar radio bursts and low-energy cosmic-rays. *Nature*, 185, 89-90.

Trottet, G., and Lantos, P., 1978. Brightness temperatures of solar coronal holes and arches at metric wavelengths and the coherency between radio and UV observations. *Astronomy and Astrophysics*, 70, 245-253.

Vinokur, M., 1968. A new radioheliograph for instant complete one-dimensional pictures at 169 MHz. *Annales d'Astrophysique*, 31, 457-463.

Wendt, H., 2008. The Contribution of the CSIRO Division of Radiophysics Potts Hill and Murraybank Field Stations to International Radio Astronomy. Ph.D. Thesis, Centre for Astronomy, James Cook University (Townsville, Aus-

tralia).

Wendt, H., Orchiston, W., and Slee, B., 2009. W.N. Christ-iansen and the development of the solar grating array. *Journal of Astronomical History and Heritage*, 11, 173-184.

Wendt, H., Orchiston, W., and Slee, B., 2011. The contribution of the Division of Radiophysics Potts Hill field station to international radio astronomy. In Orchiston, W., Nakamura, T., and Strom, R. (eds.). *Highlighting the History of Astronomy in the Asia-Pacific Region*. New York, Springer. In press.

Wild, J.P., 1967. The radioheliograph and the radio astron-omy programme of the Culgoora Observatory. *Proceedings of the Astronomical Society of Australia*, 1, 38-40.

Wild J.P., 1970. Some investigations of the solar corona: the first two years of observation with the Culgoora Radio-heliograph. *Proceedings of the Astronomical Society of Australia*, 1, 365-370.

Wild, J.P., and McCready, L.L., 1950. Observations of the spectrum of high-intensity solar radiation at metre wave-lengths. Part 1. The apparatus and spectral types of solar bursts observed. *Australian Journal of Scientific Research*, 3, 387-398.

Wild, J.P., Smerd, S.F., and Weiss, A.A., 1963. Solar bursts. *Annual Review of Astronomy and Astrophysics*, 1, 291-366.

Dr Monique Pick (Gutmann) started her research in radio astronomy in 1957 at Paris-Meudon. Under the direction of J.L. Steinberg, she partici-pated in the construction of the Nançay 3 cm array, and obtained her Ph.D. in 1961 under the direction of Jean-François Denisse. After the 1971 fire which destroyed the receiver of the 169 MHz array, she was the Project Scientist for the new Nançay Radio Heliograph until 1985. She then was the Head of the Nançay Radio Astronomy Station for eight years. Her main field of interest is the physics of the Sun and of the interplanetary medium. After a stay in 1967 at the Enrico Fermi Institute in Chicago she became involved in many space projects. Her present interest focuses on the study of coronal mass ejections and related phenomena.

Dr Jean-Louis Steinberg began working in radio astronomy with J.-F. Denisse and E.-J. Blum at the École Normale Supérieure after WW II. On his return from the 1952 URSI Congress in Sydney he began developing the Nançay radio astronomy field station, and from 1960 through to 1965 he and M. Parise led the design and construction at Nançay of 'Le Grand Radiotélescope'. In 1965, he began developing space research at Meudon Observatory. In 1960 Jean-Louis and J. Lequeux wrote a text book on radio astronomy, which was subsequently translated into English and Russian. In 1962 he was appointed Editor-in-Chief of *An-nales d'Astrophysique*, which he and his wife ran until 1969. For the next five years he was one of the two Editors-in-Chief of *Astronomy and Astro-physics*. Jean-Louis has authored or co-authored about 80 scientific publications, and has received several scientific prizes and awards.

Dr Wayne Orchiston is an Associate Professor in Astronomy at James Cook University, Townsville, Australia. His main research interests relate to Cook voyage, Australian, English, French, Indian, New Zealand and U.S. astronomical history, with emphasis on the history of radio astronomy, comets, historically-significant telescopes, solar eclipses and transits of Venus. He has published extensively, and has edited the book *The New Astronomy. Opening the Electromagnetic Window and Expanding our View of Planet Earth* (Springer, 2005). He also has a book on early Australian radio astronomy, co-authored by Woody Sullivan, which will be published by Springer in 2011. Wayne is the founder and current Vice-Chairman of the IAU Working Group on Historic Radio Astronomy.

Dr André Boischot joined the French group of radio astronomers in 1954 at the beginning of the Nançay Observatory. He was first involved with Emile-Jacques Blum in the design and construc-tion of the 32-element E-W 169 MHz solar array. He then worked with Le Grand Radiotélescope at Nançay on non-solar projects. Then, he initiated a new program to observe the Sun and Jupiter at decametric wavelengths and was co-investigator on the NASA 'Voyager' radio astronomy experi-ment where he studied the magnetospheres of the outer planets.